

Configurational splitting of the giant dipole resonance in atomic nuclei

B. S. Ishkhanov, I. M. Kapitonov, V. G. Neudachin, V. G. Shevchenko, R. A. Éramzhyan, and N. P. Yudin

Scientific-Research Institute of Nuclear Physics at the M. V. Lomonosov Moscow State University
Usp. Fiz. Nauk **160**, 57–99 (March, 1990)

The formation of the giant dipole resonance (GDR) in light ($A < 40$) atomic nuclei is studied. It is shown that the main feature of the GDR in these nuclei is configurational splitting, which is caused by the sharp drop of the deep 0s and 1p shells in 1p- and 2s, 2d-shell nuclei, respectively, and by the approximate spin-isospin SU_4 symmetry (1p-shell nuclei). As a result of this a single dipole state is not formed in light nuclei and the GDR is “spread” over groups of levels in different regions of the excitation energy. The role of this phenomenon in the system of modern ideas about the formation of collective states of nuclei is indicated and problems for further experimental and theoretical study are formulated.

1. THE BASIC MECHANISMS OF THE GIANT DIPOLE RESONANCE (GDR) IN ATOMIC NUCLEI

1. 1. Historical introduction

It is well known that the photoabsorption cross section of all atomic nuclei (except light nuclei—deuterons, tritons, the nucleus of the ^3He isotope of helium-3) has a large peak, usually called the giant dipole resonance (GDR) (Fig. 1a). In heavy nuclei (in the neighborhood of the nucleus ^{208}Pb) it lies in the region 13–14 MeV and in light nuclei it lies in the region 20–24 MeV. For medium and heavy nuclei the average energy of this peak E_d is given approximately by the empirical formula

$$E_d \approx 80A^{-1/3} \text{ MeV}, \quad (1)$$

where A is the mass number of the nucleus and the width varies from 3–4 MeV in the magic nuclei up to 6 MeV in “soft” spherical nuclei (“soft” with respect to excitation of surface vibrations). In deformed nuclei the GDR is split into two well-resolved peaks (Fig. 1b).

The existence of the GDR in nuclei was predicted theoretically by A. B. Migdal in 1945.¹ Soon after this prediction the GDR was discovered experimentally by Baldwin and Claiber, Perlman and Friedlander, and Diven and Almi.² The paper by Goldhaber and Teller,³ sometimes cited as the first theoretical description of the GDR, appeared in 1948.

The study of the nature and properties of the GDR played a leading role in the construction of models of that time of the structure and dynamics of atomic nuclei. The acute disagreement which appeared by the middle of the 1950s between the energies E_d of the “shell” GDR⁴ and the observed GDR led to the discovery of collective states and mechanisms of formation of such states on the basis of the shell model.^{5,6} The entire development of the physics of atomic nuclei during the next almost 30 years was largely connected with the study of collective states, the role of such states in different reactions, the interaction with single-particle degrees of freedom, decay modes, etc. In addition the most striking collective state in medium and heavy atomic nuclei—the dipole state—has always been a distinctive test of new approaches to the description of atomic nuclei.

A completely different (with respect to medium and heavy nuclei) structure of the GDR is realized in light nuclei. The foundations of the concept predicting qualitatively new laws for light nuclei were laid at the Scientific-Research

Institute of Nuclear Physics at Moscow State University back in the 1960s, when the entire physics of giant resonances was formulated. According to this new concept the GDR in light nuclei, in contradistinction to the GDR in medium and heavy nuclei, should extend to energies which are so much higher than the typical energies in low-energy nuclear physics that in accordance with traditional views it should not occur at all. One of the branches of the GDR predicted on the basis of this concept was observed experimentally only recently.

The main goal of this review is to uncover the new physics that makes the GDR in light nuclei qualitatively different. It seems to us that the questions studied in this review are of general importance for understanding the conditions under which collective excitations form in quantum-mechanical many-body systems.

1.2. Formation of the GDR in medium and heavy nuclei

All modern data on stripping and pickup reactions,⁸ elastic and inelastic scattering of electrons,⁹ and quasielastic knockout of protons from nuclei by electrons¹⁰ and protons¹¹ in aggregate leave no doubt that in the first (and good) approximation an atomic nucleus is a Fermi gas of nucleons moving in the self-consistent nuclear field. We shall call this nuclear field the shell potential.

In the simplest case the shell potential is the Hartree potential. Obviously the questions of the form of the shell potential and therefore the structure of the nuclear shells are very important questions. Once again the modern data in aggregate indicate that the single-particle levels near the Fermi surface can be regarded as levels in a static local potential with a diffuse boundary (this potential is sometimes called the Woods-Saxon potential).

It turns out, however, that the local statistical potential is not useful for reproducing the “deep,” i.e., far from the Fermi surface, single-particle levels: these levels lie much deeper than this potential predicts.^{10,11} We shall see below that this feature of nuclear shells in light nuclei is responsible for one of the most important phenomena—*configurational splitting of the GDR*.

We shall first discuss the question of the formation of the GDR in medium and heavy nuclei. We start by studying the double magic nuclei ^{90}Zr , ^{48}Ca , etc. We shall assume first that all nuclear interactions between nucleons reduce to a

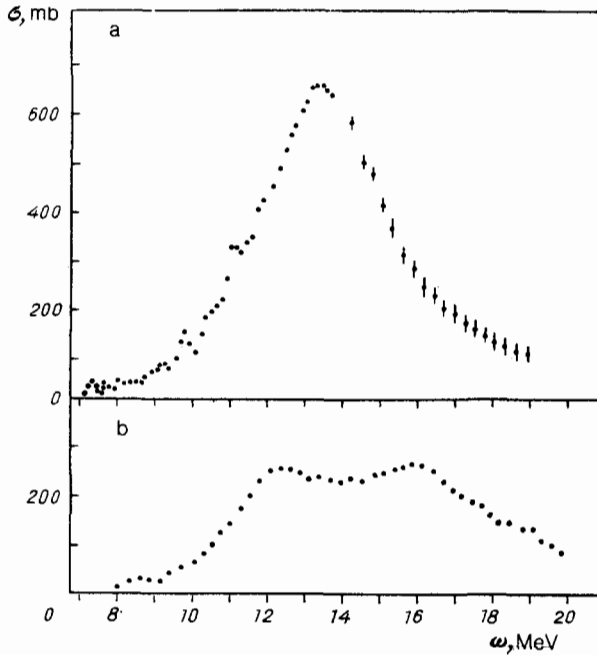


FIG. 1. The total cross section for absorption of γ -quanta as a function of their energy ω for the nuclei ^{208}Pb (Ref. 24) (a) and ^{154}Sm (Ref. 24) (b).

shell potential. In this model the simplest excited states of magic nuclei are the particle-hole states (configurations) $|\text{ph}\rangle$, obtained by transferring one nucleon from the filled shells (and, therefore, forming a vacancy—"hole"—in them) into the empty shells:

$$|\text{ph}\rangle = a_p^+ a_h |0\rangle, \quad (2)$$

where $|0\rangle$ is the ground state of the filled shells and a_p^+ and a_h are operators creating a nucleon in an empty shell and annihilating a nucleon in a filled shell. More precisely

$$|\text{ph}\rangle = |\bar{n}_1 \bar{l}_1 \bar{j}_1 n_2 l_2 j_2 J T\rangle = |\bar{j}_1 j_2 J T\rangle, \quad (3)$$

where $n l j$ are the quantum numbers of a level in a spherically symmetric potential (the type of potential encountered most often), the overbar on the indices $n l j$ denotes a "hole," and J and T are the total angular momentum and the isospin. In nuclei with zero angular momentum $J = 1$ (the GDR is associated with the absorption of a dipolar photon); in nuclei with $N = Z$ (N and Z are the numbers of neutrons and protons) $T = 1$; we shall ignore here the details of the isotopic structure of medium and heavy nuclei (see Ref. 12). The excitation energies E_{ph} of particle-hole configurations are given by the obvious formula

$$E_{\text{ph}} = \varepsilon_p - \varepsilon_h, \quad (4)$$

where $\varepsilon_{p,h}$ are the energies of the particle and hole states.

More complicated excited states are states of the type $(2p, 2h)$ (two particles—two holes), $(3p, 3h)$, etc., which are formed when two, three, etc., nucleons are transferred from filled shells into empty shells.

Because of the single-nucleon nature of the interaction of γ -quanta with a nucleus, in the shell model the GDR is connected with particle-hole configurations of neighboring shells⁴ and in heavy nuclei its energy should equal the splitting between the shells, i.e., 6–8 MeV, instead of the observed

13–14 MeV. This is the sharp discrepancy mentioned above, which appeared in the theory in the mid-1950s. The solution to this problem^{5,6} (also found in Ref. 7) was connected with the recognition of the fact that the entire nuclear interaction in principle cannot be reduced to a self-consistent potential and that the remaining part of the interaction—the residual interaction—can lead to nontrivial effects. For this reason, the problem of the GDR is formulated as follows: find the excitation spectrum of the model Hamiltonian

$$\hat{H} = \hat{H}_0 + \hat{V} \quad (5)$$

taking all configurations ph , $2p2h$, etc., into account (naturally, the configurations have the required angular momenta J, T). Here H_0 is the "zeroth-order" approximation of the Hamiltonian

$$\hat{H}_0 |\text{ph}\rangle = E_{\text{ph}} |\text{ph}\rangle, \quad (6)$$

and \hat{V} is the residual-interaction operator which "operates" only in the excited state. We shall discuss the effects of the residual interaction in the ground state in Sec. 1.4. The explicit formulas for the amplitudes $\langle p'h' | \hat{V} | \text{ph} \rangle$, $\langle p'h' | \hat{V} | 2p2h \rangle$, etc., depend on the type of residual interaction.¹³

The excitation spectrum of the Hamiltonian (5) is found by diagonalizing the energy matrix $\|H\|$:

$$H = \begin{vmatrix} \langle p'h' | \hat{H} | \text{ph} \rangle & \langle p'h' | \hat{H} | 2p2h \rangle & \dots \\ \langle 2p'2h' | H | \text{ph} \rangle & \langle 2p'2h' | H | 2p2h \rangle & \dots \\ \dots & \dots & \dots \end{vmatrix} \text{ etc.} \quad (7)$$

The diagonalization procedure is complicated by the fact that the single-particle shell Hamiltonian has a continuous spectrum. In practically all subsequent calculations of the properties of the GDR the continuous spectrum is neglected (see Sec. 1.4). As a result of this the single-particle basis and therefore the basis of ph -, $2p2h$ -, etc., configurations becomes finite. Even in this case, however, it is impossible, at least at the present, to take all discrete states of the basis into account. For this reason, new model assumptions must be introduced already in the model formulation of the problem itself. An important achievement of the theory is that in spite of the fact that the problem of diagonalizing the Hamiltonian (5) cannot be solved exactly the main features of the GDR are now understood not only qualitatively, but in part quantitatively also.

The residual interaction plays a double role in the formation of the excitation spectrum of the Hamiltonian (5). On the one hand, it gives rise to "scattering" of particles by holes, in which process the total number of particles and holes is conserved, while on the other it creates and annihilates particle-hole pairs and therefore couples configurations in the chain

$$\text{ph} \rightleftharpoons 2p2h \rightleftharpoons 3p3h \rightleftharpoons \dots \text{ etc.} \quad (8)$$

We shall first clarify the particle-hole scattering effects. We shall study the case of ph configurations, which is most important in the problem of the GDR. In diagonalizing the Hamiltonian (5) in the ph basis the following two circumstances are of fundamental importance. First, ph configurations for which the amplitudes $d_{\text{ph}} = \langle \text{ph} | D | 0 \rangle$ of the dipole transitions are large (D is the electric dipole moment opera-

tor of the nucleus) are approximately energy degenerate. This feature of the GDR problem is connected in an obvious way with the form of the shell potential (see the discussion of this question for the case of nonmagic and light nuclei). Second, the amplitudes $\langle p'h' | V | ph \rangle$ of the interactions of these "strong" particle-hole states approximately factor

$$\langle p'h' | V | ph \rangle = \kappa d_{p'h} d_{ph}, \quad (9)$$

where κ is a positive constant.

Under these conditions, as is easily verified,⁶ the residual interaction forms from the "strong" ph configurations a coherent dipole state

$$|d\rangle \sim \sum_{ph} d_{ph} |ph\rangle \quad (10)$$

with substantially nontrivial properties. It is precisely this state that exhausts in an obvious fashion all dipole transitions in the nucleus (and therefore forms the GDR) and is shifted upwards in energy by the amount

$$\Delta E = \kappa \sum_{ph} (d_{ph})^2. \quad (11)$$

Taking into account the "weak" configurations, i.e., ph configurations with small amplitudes d_{ph} , does not change this conclusion overall, but it does lead to some fragmentation of the dipole state.

Configurations of the type 2p2h and more complicated configurations above the Hartree-Fock vacuum cannot be excited directly by γ -quanta and affect the GDR only indirectly. The explanation of the effects of these configurations was a big achievement of the theory.¹³⁻¹⁷ It turned out that they do not change the average energy of the particle-hole GDR and in practice form only its width—the intermediate and fine structure, if more important factors of the type studied in this review, configurational splitting or static deformation, are not significant. The reason that the more complicated configurations have such a "limited" effect on the GDR is that, first, the ph interaction "induced" by them cannot have the factorized form (9) and, second, under reasonable assumptions about the randomness of the phase factors of the amplitudes $\langle ph | \hat{V} | 2p2h \rangle$ is in general diagonal in the ph configurations.

We shall give a formal explanation of this assertion. The effective cross section $\sigma(\omega)$ for absorption of γ -quanta by a nucleus which, for simplicity, we shall assume to be spinless, is given by the formula

$$\sigma(\omega) = 4\pi^2 \alpha \omega \operatorname{Im} \langle 0 | \hat{D} \hat{G}(\omega) \hat{D} | 0 \rangle, \quad (12)$$

where

$$\hat{D} = \frac{N}{A} \sum_{i=1}^Z \hat{z}_i - \frac{Z}{A} \sum_{i=Z+1}^A \hat{z}_i \quad (13)$$

is the dipole moment operator of the nucleus (Z and N are the numbers of protons and neutrons and \hat{z}_i is the z coordinate of the i th nucleon), $\alpha = 1/137$ is the fine structure constant, and $\hat{G}(\omega)$ is the total propagator (Green's function) of the Hamiltonian (5):

$$\hat{G}(\omega) = \frac{1}{\omega - \hat{H} + i\delta}. \quad (14)$$

Since it is projected on the ph subspace of the total Hilbert space of the basis states the propagator $\hat{G}(\omega)$ can be written in the form¹⁸

$$\hat{G}(\omega) = \frac{1}{\omega - \hat{H}_{ph} - \hat{V} \hat{G}_{spah} \hat{V} + i\delta}, \quad (15)$$

where \hat{H}_{ph} is the Hamiltonian (5) in the ph subspace, $\hat{G}_{2p2h}(\omega)$ is the total propagator in the subspace of the configurations 2p2h, 3p3h, etc., and the operator \hat{V} connects ph configurations with more complicated configurations.

In the general case the cross section (12) is a strongly fluctuating function of the frequency ω of the photon. It therefore makes sense to average this cross section over some energy interval I . This averaging is usually performed with the help of the weighting function

$$\rho_I(\omega, \omega') = \frac{1}{\pi} \frac{I/2}{(\omega - \omega')^2 + (I/2)^2}. \quad (16)$$

As a result, for the average cross section $\sigma_I(\omega) = \int \rho_I(\omega, \omega') \sigma(\omega') d\omega'$ we obtain

$$\sigma_I(\omega) = 4\pi^2 \alpha \omega \operatorname{Im} \langle 0 | \hat{D} \hat{G}(\omega + i\frac{I}{2}) \hat{D} | 0 \rangle. \quad (17)$$

If the density of states ρ of states of the type 2p2h, 3p3h, ... is sufficiently high ($\rho \gg 1/I$), it may be assumed that

$$\begin{aligned} \langle p'h' | \hat{V} \hat{G}_{spah}(\omega + i\frac{I}{2}) \hat{V} | ph \rangle &= \delta_{p'h',ph} \langle ph | \hat{V} \hat{G}_{spah}(\omega + i\frac{I}{2}) \hat{V} | ph \rangle \\ &= \delta_{p'h',ph} \left(\Delta_{ph}(\omega) - i \frac{\Gamma_{ph}(\omega)}{2} \right), \end{aligned} \quad (18)$$

where

$$\Delta_{ph}(\omega) = \sum_{sp2h} \frac{\omega - \omega_{sp2h}}{(\omega - \omega_{sp2h})^2 + (I/2)^2} |\langle ph | \hat{V} | 2p2h \rangle|^2, \quad (19')$$

$$\Gamma_{ph}(\omega) = 2\pi \sum_{sp2h} \frac{I/2\pi}{(\omega - \omega_{sp2h})^2 + (I/2)^2} |\langle ph | \hat{V} | 2p2h \rangle|^2. \quad (19'')$$

The cross section $\sigma_I(\omega)$ correspondingly assumes the form

$$\sigma_I(\omega) = 4\pi^2 \alpha \omega \sum_k \frac{|\langle k | \hat{D} | 0 \rangle|^2 \Gamma_k(\omega)/2}{(\omega - \omega_k - \Delta_k(\omega))^2 + (\Gamma_k(\omega)/2)^2}, \quad (20)$$

where $|k\rangle$ and ω_k are the eigenfunctions and eigenvalues of the particle-hole Hamiltonian \hat{H}_{ph} . Thus we can see that under the very reasonable assumption (18) (randomness of the amplitudes coupling the ph and 2p2h states) the 2p2h and more complicated configurations merely shift and broaden the particle-hole states.

We shall now study the formation of the GDR in nuclei with unfilled shells. For definiteness we shall study nuclei with one unfilled (valence) shell. The new elements in the formation of the GDR in such nuclei are as follows.

a) There are two types of transitions—from the valence shell into an empty shell and from a filled shell into the valence shell. We shall term transitions of the first kind type A and transitions of the second kind type B:

b) The Fermi surface of the nucleon gas is "diffuse," i.e., in the ground state of the nucleus nucleons fill with definite probabilities all states of the valence shell:

c) The ground state has a genealogical structure, i.e., when a nucleon is removed from the valence shell or when a nucleon is added to the valence shell an entire set of states of the nucleus ($A + 1$) is excited with definite probabilities. The genealogical structure is given by the parentage coefficients given by the relations

$$\hat{a}_{j_1 m_1} |\Psi_0\rangle = N^{1/2} \sum_{s_{A-1}} \langle s_{A-1}, j_1 | \Psi_0 \rangle \times \langle J_{s_{A-1}} M_{s_{A-1}} j_1 m_1 | J_0 M_0 \rangle |s_{A-1}\rangle \quad (21)$$

and

$$\hat{a}_{j_1 m_1}^+ |\Psi_0\rangle = (N+1)^{1/2} \sum_{s_{A+1}} \langle \Psi_0, j_1 | s_{A+1} \rangle \times \langle J_0 M_0 j_1 m_1 | J_{s_{A+1}} M_{s_{A+1}} \rangle |s_{A+1}\rangle, \quad (22)$$

where $\langle s_{A-1}, j_1 | \Psi_0 \rangle$ is the genealogical separation coefficient describing the separation of the j_1 nucleon from the ground state $|\Psi_0\rangle$ with excitation of the state $|s_{A-1}\rangle$ of the final nucleus; the coefficient $\langle \Psi_0, j_1 | s_{A+1} \rangle$ has an analogous meaning; N is the number of nucleons in the valence shell; and, $J_0 M_0, J_{s_{A\pm 1}}, M_{s_{A\pm 1}}$ are the angular momenta and their projections for the states $|\Psi_0\rangle, |s_{A\pm 1}\rangle$.

In general it is much more difficult to analyze theoretically the GDR in nonmagic nuclei than in magic nuclei. In medium and heavy nuclei the theoretical analysis is greatly simplified by the fact that the pairing interaction between nucleons plays the main role in the formation of the ground state of the nucleus. As a result of this the genealogical structure of the ground states of medium and heavy nuclei is, as a rule, trivial (in even-even nuclei only one state of the final nucleus is excited when a nucleon is removed from the valence shell), and the apparatus of the theory of superconductivity¹⁹ (a detailed discussion is given in Ref. 16) formally reduces the problem of the GDR in nonmagic nuclei to that of the GDR in magic nuclei.

The general result of numerous calculations of the GDR in medium and heavy nuclei reduces to the following: in these nuclei the formation of the GDR occurs by the mechanism operating in magic nuclei—a coherent dipole state, which is strongly shifted (by 7–8 MeV) upwards in energy, is formed (because the shells are unfilled it is formed by a significantly larger number of configurations). States whose structure is more complicated than the particle-hole structure are responsible for the width of the GDR.

1.3. Characteristic features of the formation of the GDR in light nuclei

We shall term nuclei which are lighter than the calcium nucleus (with $A \leq 40$), i.e., 1p- and 2s-, 2d-shell nuclei, light nuclei. To give a better idea of the distinctiveness of the GDR in light nuclei we shall give a, so to speak, “bird’s eye view” of the GDR.

In medium and heavy nuclei the GDR is determined not by the individual (structural) but rather by the average characteristics of the nuclei. Indeed, the collective particle-hole dipole state forming the basis of the GDR is a coherent superposition of many ph configurations, and its properties are virtually identical in all nuclei. Furthermore, the decay properties of the GDR in these nuclei are connected with the fragmentation of the dipole state into an enormous number of 2p2h and more complicated configurations, so that they too reflect only the average characteristics of the nuclei. As a

result the picture of the GDR in medium and heavy nuclei is quite monotonous, and the monotony is broken only by the splitting of the resonance owing to deformation of the nucleus and isospin splitting. Thus in interpreting the GDR it is entirely natural to use the model of a nucleon Fermi gas with pairing (nuclear variant of the Bardeen–Cooper–Schrieffer model¹⁹), in which all structural aspects of the nucleus vanish and only one nuclear parameter remains—the Fermi momentum p_F .

The situation for light nuclei is completely different. Here the Fermi gas philosophy is completely inadequate, and the theory of the GDR must be constructed based on the theory of nuclear structure which in the first and good approximation is described by the many-body variant of the shell model. The general physical basis for the distinctiveness of the GDR in light nuclei is ultimately connected with the nontrivial features of the mean (Hartree-Fock) field and reduces to the following.

First, because of the sharp lowering of the deep single-particle energy levels transitions of the types A and B are strongly distinguished. Because of this, in many cases the energy spread of the configurations reaches 10–15 MeV and greater.

Second (and this is especially important for 1p-shell nuclei), the self-consistent mean potential depends strongly on the quantum number $[f]$ of Young’s scheme (a more detailed discussion is given in Sec. 3); this quantum number characterizes the permutational symmetry of the spatial variables of the shell configuration.

In reality, under these conditions it is pointless to analyze the GDR in terms of single-particle shells. It is more convenient to indicate directly the shell configuration and its Young scheme. The splitting of the configurations according to Young’s schemes reaches 15–16 MeV in 1p-shell nuclei. We shall term the aggregate of physical phenomena associated with these two features of light nuclei *configurational splitting*.²⁰

Third, in light nuclei the genealogical structure of the ground and excited states is extremely rich. In 1p-shell nuclei, for example, the expansions^{21,22} include the states $|S_{\alpha\pm 1}\rangle$ lying in the interval 20–30 MeV.

Finally, fourth (and this is an extremely happy circumstance for the analysis of the GDR), in light nuclei the density of states which are more complicated than particle-hole states turns out to be low in the region of the GDR. The decay properties of the GDR are therefore largely determined by the initial ph configurations.

The large spread produced by the first two factors in the energy of the initial configurations results in the fact that in light nuclei a single dipole state is not formed as a rule and the GDR essentially remains “spread” over strongly separated separate groups of ph states from which “local” dipole “substates” can form. The formation of these groups and their decay properties are very sensitive to the energy of the deep holes, i.e., the binding energy of the nucleons in the nearest closed shell.

It is thus obvious that compared with medium and heavy nuclei the GDR in light nuclei, first, forms according to different principles and, second, it contains much richer information. *The heart of the new physics of the GDR in light nuclei is configurational splitting.*

The theoretical methods for analyzing the GDR in light

nuclei are based on the many-body shell model. The necessary elements of this model²¹ are: 1) the shell Hamiltonian

$$\hat{H} = \hat{H}_0 + \hat{V}, \quad (23)$$

where \hat{H}_0 is the Hamiltonian of independent nucleons in the valence shell, moving in the mean field generated by the nucleons of the filled shells and \hat{V} is the effective pair interaction between the valence nucleons; 2) the "configurations," i.e., the set of wavefunctions of independent valence nucleons that have the correct conserved quantum numbers. The single-particle levels of the nucleons in the field of the "core"—the nucleons in the filled shells—are obtained, as a rule, from experiment; the radial parts of the single-nucleon wave functions are often assumed to be oscillatory. The solution of the many-body problem of finding the ground state and the excitation spectrum reduces to diagonalizing the Hamiltonian (24) in some basis of configurations. The larger the basis, the more accurate the solution of the problem is. We shall indicate as an example the scheme of a shell calculation of the GDR in the ^{12}C nucleus. The Hamiltonian \hat{H}_0 in this case describes the independent nucleons in the $1p$ shell, moving in the field of the ^4He nucleus. To find the ground state the Hamiltonian \hat{H} is diagonalized in the basis of the configurations.

$$|0s^4 1p^8 [f] LST=0, J=0\rangle, \quad (24)$$

where $[f]$ is Young's scheme (see Sec. 3 below), LST are the total orbital, spin (the LS coupling scheme), and isospin angular momenta, and J is the total angular momentum of the nucleus. The configurations are distinguished by the quantum numbers $[f]$ and LS. In finding the GDR in the ^{12}C nucleus the Hamiltonian \hat{H} must be diagonalized in an analogous fashion in the basis of configurations

$$\begin{aligned} |0s^4 1p^7 [f] (LST)^\pi, \alpha (2s, 2d): J^\pi T\rangle, \\ |0s^3 1p^9 [f^1] (LST): J^\pi T\rangle, \end{aligned} \quad (25)$$

with $J^\pi = 1^-$ and $T = 1$.

We shall call calculations of this type calculations by the BSM($1\hbar\omega$) (Bound Shell Model) method; the notation $1\hbar\omega$ means that all configurations obtained from the ground state by transferring a nucleon into a neighboring shell are taken into account. There are, however, a number of technical questions (for example, the separation of center-of-mass excitations) as well as fundamental questions (the problem of the effective interaction) in the practical implementation of this program. Shell calculations nonetheless give results which are in reasonably good agreement with experiment.

Good results are also obtained by reducing the BSM($1\hbar\omega$) basis to a set of states of the type

$$\begin{aligned} a_p^+ |s_{A-1}\rangle, \\ a_h |s_{A+1}\rangle, \end{aligned} \quad (26)$$

where a_p^+ and a_h are operators creating a nucleon in an empty shell and annihilating a nucleon in a filled shell; $|s_{A \pm 1}\rangle$ denotes the states of $A \pm 1$ nuclei which are genealogically related with the ground states (i.e., these states are excited when a nucleon is removed from or added to the valence shell).

For the ^{12}C nucleus, for example, this approximation

means that the Hamiltonian (23) must be diagonalized in the basis

$$\begin{aligned} |0s^4 1p^7 \alpha J_1 = \frac{1}{2} T_1 = \frac{1}{2}, (2s, 2d): J^\pi = 1^-, T=1\rangle, \\ |0s^3 1p^9 \beta J_1 = \frac{1}{2} T_1 = \frac{1}{2}: J^\pi = 1^-, T = 1\rangle, \end{aligned} \quad (27)$$

where α and β are additional (to J_1 and T_1) indices of the states of nuclei with $A = 11$ and 13 , genealogically coupled with the ground state of the ^{12}C nucleus.

The basis of configurations can be further reasonably reduced by working with configurations of the type

$$\begin{aligned} a_p^+ |\overline{s_{A-1}}\rangle, \\ a_h |\overline{s_{A+1}}\rangle, \end{aligned} \quad (28)$$

where the overbar means that wave packets which exhaust the entire genealogy of the ground state are used instead of the set of states $|s_{A \pm 1}\rangle$:

$$\begin{aligned} |\overline{s_{A-1}}\rangle &= \sum_{s_{A-1}} \langle s_{A-1}, j_1 | \Psi_0 \rangle |s_{A-1}\rangle, \\ |\overline{s_{A+1}}\rangle &= \sum_{s_{A+1}} \langle \Psi_0, j_1 | s_{A+1} \rangle |s_{A+1}\rangle. \end{aligned} \quad (29)$$

The approximations (28) and (29) are a natural physical extrapolation of the particle-hole approximation for magic nuclei to nonmagic nuclei. This makes it clear that the approximation (27) (we are no longer talking about the BSM ($1\hbar\omega$) approximation) takes into account the contribution of a number of configurations of the type $2p2h$ to the GDR.

The approximation (29) is valid when the shift ΔE , produced by the residual interaction, in the energy of the GDR is much greater than the energy spread of the states of $(A \pm 1)$ nuclei, exhausting the genealogy of the starting nucleus.

1.4. The GDR in the nuclei ^{208}Pb and ^{16}O

In this section we shall illustrate for the example of the GDR in ^{208}Pb and ^{16}O nuclei the "operation" of the theoretical apparatus described in Secs. 1.2–1.4. The ^{208}Pb nucleus is a double-magic heavy nucleus. The GDR in this nucleus, calculated in the ph approximation taking into account $2p2h$ configurations and measured experimentally, is presented in Fig. 2. As one can see from this figure the theory describes satisfactorily the gross structure of the absorption curve. Nonetheless there is still no direct experimental confirmation of the particle-hole nature of the GDR in this nucleus. This situation is connected with the fact that the particle-hole configurations in medium and heavy nuclei are "hidden": the decay properties of the GDR are determined not by the ph configurations, but rather by an enormous number of $2p2h$ and more complicated configurations, which have no relation to the process of absorption of γ -quanta. It appears that the only way to obtain direct experimental confirmation of the ph nature of the GDR in heavy nuclei is to study the form factors of the GDR. Indeed, if the contribution of the GDR to inelastic scattering of electrons with sufficiently high transferred momenta q ($q \gtrsim 0.5 \cdot 10^{13} \text{ cm}^{-1}$) could be determined, then it would be possible to judge confidently the validity of the ph approximation by comparing

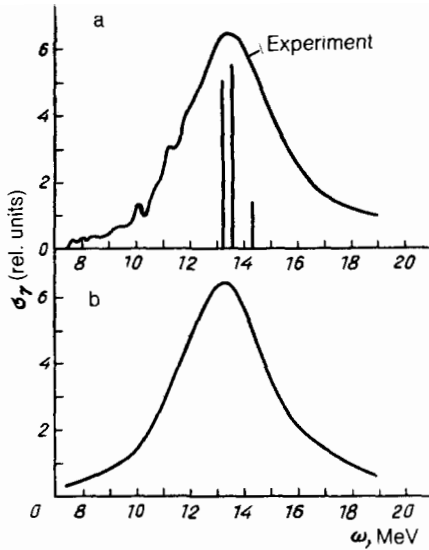


FIG. 2. The γ -quantum absorption cross section calculated for the nucleus ^{208}Pb in different approximations²⁴: ph (a) and ph + 2p2h (b). The measured cross section is presented for comparison.

the measured form factors with the form factors computed using the ph theory.

In this connection we stress the uniqueness of the GDR in ^{16}O , for the example of which the correctness of the mechanisms of the GDR studied above can be checked directly. The computed²² and experimental⁶² absorption curves for this nucleus are shown in Fig. 3. It is obvious from the figure that the gross structure of the experimental curve—two peaks, one at 22.3 MeV and the other at 24.4 MeV—is explained very well in the ph-approximation. True, the theoretical peaks (22.7 MeV and 25.4 MeV) are shifted somewhat relative to the experimental peaks, but this discrepancy can be explained by small imperfections of the theory (the form of the residual interaction, the form of the shell potential, etc.). The wavefunctions of these states are superpositions of five ph-configurations excited by γ -quanta:

$1\bar{p}_{3/2}2s_{1/2}$, $1\bar{p}_{1/2}2s_{1/2}$, $1\bar{p}_{3/2}2d_{5/2}$, $1\bar{p}_{1/2}2d_{3/2}$, $1\bar{p}_{3/2}2d_{3/2}$ (we note that the dominant configurations for the 22.7 MeV and 25.4 MeV levels are $1\bar{p}_{3/2}2d_{5/2}$, and 25.4 — $1\bar{p}_{3/2}2d_{3/2}$, respectively). A detailed and in-depth check of the ph-structure of the GDR in this nucleus was performed based on extensive data on the partial cross sections of (γ, p_i) reactions, where the index i denotes low-lying states of the final nucleus ^{15}N ($1/2^-$, $3/2^-$, $1/2^+$, $5/2^+$, $3/2^2$), and also on the angular distributions of the photonucleons²⁴ and the differential cross sections for radiative capture of polarized protons.²⁵ It was found that these data as a whole are consistent with the configurational composition of particle-hole states obtained by Gillet.²² An explanation was also found for the fact that the angular distributions of nucleons measured in different parts of the GDR are identical even though the configurational composition of these regions is different. However, the existence of fine structure in the GDR in the ^{16}O nucleus, “not provided” by the ph-approximation, and the fact that the GDR decays into nonhole states of the final nuclei ($1/2^+$, $5/2^+$, $3/2^+$ states) indicate that states which are more complicated than particle-hole states play a definite role in the GDR in the ^{16}O nucleus. Taking these more complicated states into account more accurately²⁴ makes it possible to explain not only the fine structure of the GDR but also characteristic features of the GDR, such as the lower anisotropy of the angular distributions of the photonucleons for the 21.0, 22.6, and 24.6 MeV lines.

1.5. Additional general questions regarding the formation of the GDR

The GDR in atomic nuclei is a complex phenomenon in which all the fundamental model questions of low-energy nuclear physics are focused. In this section we shall indicate with virtually no discussion a number of such questions which are important but not determining for the problem of the GDR. Each question, generally speaking, deserves a special review.

1.5.1. Form of the residual (effective) interaction. Many variants of the residual interaction exist. These variants either crystallize out in the course of shell calculations—Ro-

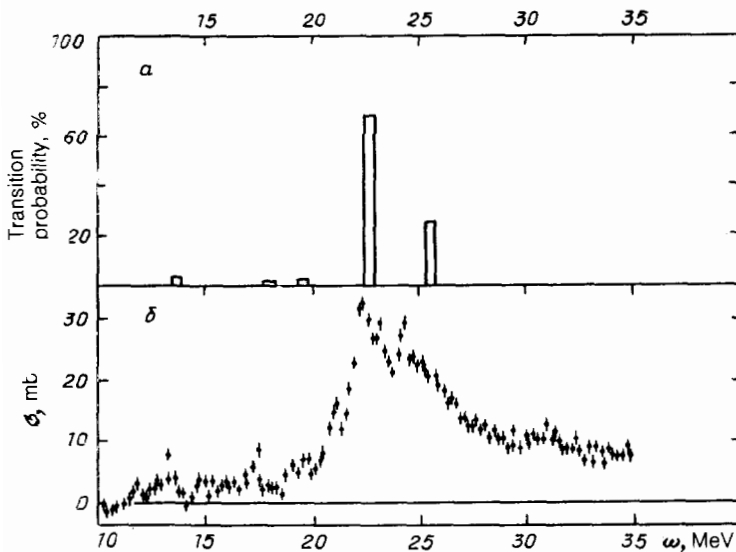


FIG. 3. The cross section for the absorption of γ -quanta by the ^{16}O nucleus calculated in the ph approximation (Ref. 22b) (a) and the measured cross section (Ref. 62) (b).

senfeld's, Soper's, Gillet's, and Skyrme's interactions,²⁶ etc.—or they are obtained by parametrization of the particle-hole interaction (Fermi-liquid theory¹³) or, finally, they are found from the G-matrix theory, relating the residual interaction with a realistic nucleon-nucleon interaction.²⁷

If separate details—threshold phenomena, properties of separate levels, etc.—are excluded, then, as calculations show, the problem of the GDR is on the whole virtually independent of the type of residual interaction.

1.5.2. The role of the continuous spectrum of single-particle states. In studying the formation of the GDR we assumed that a nucleon is transferred from a filled state into a free discrete state in a neighboring shell, for example, the transfer (transition) $1p \rightarrow 2s, 2d$. In the case indicated, however, the transitions $1p \rightarrow \varepsilon s, \varepsilon d$, where ε is the energy of the nucleon in the continuum, occur. The problem of taking the effects of the continuum into account correctly became acute in nuclear physics in the mid 1960s. A large number of articles and reviews are devoted to this problem (see, for example, Ref. 28). The overall result of the study of the effects of the continuous spectrum reduces to the following. The continuous spectrum is significant primarily in those cases when the partial widths or the interference of direct and resonance processes are calculated. Neglecting the continuous spectrum does not change fundamentally the results of the calculation of the GDR with a discrete set of states.

In summarizing these two sections we note that in a quantitative calculation of the properties of the GDR the restrictions imposed on the form of the residual interaction by the condition that they be consistent¹³ with the shell potential as well as the continuous spectrum must, of course, be taken into account correctly, especially since in forming many collective nuclear states (and the GDR) there is a tendency to increase the role of high-energy states of the continuum.¹³

1.5.3. The decay properties of the GDR: ejection of nucleons and complex fragments. Taking into account systematically the ejection of particles in the decay of the GDR is a very difficult dynamical problem and it can be done only within the framework of unified theories of nuclear reactions.²⁹ Over the last ten years significant progress in understanding the decay properties of highly excited nuclear states has been achieved based on the theory of preequilibrium (precompound) decay.^{18,30} From the viewpoint of the time-dependent variant of this theory of decay the GDR occurs as follows. The absorbed γ -quantum directly excites only particle-hole configurations. These configurations can either undergo nucleon (or some other) decay or they can transform into a more complicated 2p2h configuration. In the second case—the appearance of a more complicated 2p2h configuration—everything is repeated and terminates either with the nucleus decaying out of the 2p2h configuration or with an even more complicated 3p3h configuration appearing, etc. The required formulas for the probability of decay of a nucleus at each stage of this process can be found in Refs. 18 and 30.

The calculations of the decay properties of the GDR based on the formulas of the unified theories^{18,30} unavoidably lead to the problem of making a sufficiently accurate choice of the residual interaction and the wave functions of the continuous spectrum, on which the probability of decay depends quadratically. For this reason in many cases it is

more convenient and simpler to use the R-matrix theory to find the decay probabilities.³¹ This theory describes well the decay of independent resonating levels and therefore the basic features of the decay of the GDR. In the R-matrix theory the partial decay width $\Gamma_{\lambda a}$ of a level λ in the channel a is given by the formula

$$\Gamma_{\lambda a} = 2k_a P(k_a) \gamma_{\lambda a}^2, \quad (30)$$

where k_a is the wave vector of the relative motion of the fragments, $P(k_a)$ is the penetrability factor for the Coulomb and centrifugal barriers, $\gamma_{\lambda a}^2$ is the reduced width which is proportional to the squared parentage coefficient of separation of the level into fragments:

$$\gamma_{\lambda a}^2 = \frac{1}{2\mu R} |\varphi(R)|^2 |\langle a | \psi_\lambda \rangle|^2; \quad (31)$$

$\varphi(R)$ is the wavefunction of the relative motion of the fragments, R is the distance between the centers of the fragments at which they touch, $|\langle a | \psi_\lambda \rangle|^2$ is the squared parentage coefficient multiplied by the combinatorial factor for the formation of a fragment from A nucleons in the nucleus, and μ is the reduced mass.

1.5.4. The role of correlations in the ground state. In the preceding qualitative analysis (see Secs. 1.2–1.4) we actually studied the effects of interaction in the final state, i.e., the interaction of particles and holes generated by the γ -quantum.

Meanwhile, an interaction capable of scattering and generating ph pairs will unavoidably distort the Hartree-Fock vacuum. This distortion of the Hartree-Fock vacuum is partially taken into account by the random phase approximation (RPA).³² From the viewpoint of the physics the RPA corresponds to taking into account in the diagonalization scheme an admixture to the ground state of configurations of the type

$$\hat{a}^\dagger |0\rangle, \quad (32)$$

where

$$\hat{a} = \sum_{ph} d_{ph} a_p^\dagger a_h \quad (33)$$

and $|0\rangle$ is the Hartree-Fock vacuum.

Long-range correlations in the ground state are significant in different many-body problems—in the analysis of plasma oscillations of the degenerate electron gas, photoionization of atoms, etc.³³ In nuclear physics they are very important in calculations of the properties of low-lying collective states $2^+, 3^-$. In the GDR problem, however, because of the structure of the residual interaction such correlations on the whole play a secondary role, though in discussing a number of collective characteristics of the GDR they must be taken into account (for example, in the analysis of the dipole sum rule).

1.5.5. Exchange currents. Direct excitation of the configuration 2p2h. Exchange currents do not play a significant role in the region of the GDR, since in the long-wavelength approximation the operator describing the interaction of the atomic nucleus with the electromagnetic field is a single-particle operator. In the region of photon energies ω greater than 100 MeV, however, exchange currents play a very significant role, giving rise to two-nucleon absorption of γ -quanta.

The direct excitation of 2p2h states occurs owing to ex-

change currents and falls outside the RPA (higher-order RPA approximations). Both these mechanisms for direct excitation of the 2p2h configurations have virtually no effect in the region of the GDR.

2. DEEP HOLES AND THE STRUCTURE OF THE GDR IN LIGHT NUCLEI

2.1. The problem of deep holes in light nuclei

By deep levels and correspondingly deep holes we shall mean the single-particle shell levels lying below a filled (or the last filled) shell. In 2s, 2d-shell nuclei these are $\overline{0s}$, $\overline{1p}$ hole levels and in 1p-shell nuclei they are $\overline{0s}$ levels. The problem of deep holes arose and attracted attention 15 to 20 years ago, after ($\overline{0s}$, $\overline{1p}$)-levels of 1p- and 2s, 2d-shell nuclei were identified in (e,e'p) (Ref. 9) and (p,2p) (Ref. 10) experiments. It turned out that the binding energy of these levels is significantly higher than predicted by the conventional static shell potential with a depth of 45–50 MeV. The scales of the discrepancy can be judged, for example, based on the fact that according to modern data (Fig. 4) the binding energy of the 0s state has a tendency to reach the asymptotic value $E(0s) \approx 60$ MeV (for $A > 40$), while the binding energy of the 1p state has a tendency to reach the value $E(1p) \approx 40$ MeV.

The binding energy of deep states depends approximately linearly on the number of valence nucleons. For example, when a neutron shell is filled the deep levels of the proton shell shift downwards by an amount ΔE given by the formula

$$\Delta E \approx \epsilon N, \quad (34)$$

where N is the number of neutrons in the valence shell, and

$$\epsilon_{0s} = 4 \text{ MeV}, \quad \epsilon_{1p} = 2 \text{ MeV} \quad (35)$$

respectively for 1p- and 2s, 2d-shell nuclei.

Another feature of deep holes which is important for GDR is their very strong fragmentation, owing to the fact that they are coupled to p, 2h, and more complicated states. For example, the effective width of the $\overline{0s}$ hole state in ^{12}C and ^{16}O nuclei reaches 25 MeV, while the effective width of the 1p state in (2s,2d)-shell nuclei reaches 15–20 MeV.

There is still no adequate quantitative understanding of the energy of deep holes and the mechanisms by which they fragment. Hartree-Fock calculations of the single-particle potential with the Skyrme N - N interaction leads to an E -dependent (i.e., energy dependent) shell potential.³⁴ Such potentials reproduce well the energies of deep states and their wavefunctions (more accurately, the momentum distributions³⁵). It is possible that the introduction of E -dependent potentials in shell theories is in fact the solution of the problem of deep holes. It is also possible that the problem of the fragmentation of deep holes will make it necessary to take into account effects of the Mahan-Noziere type³⁶ occurring in metals.

2.2. Deep holes and the structure of the GDR. General analysis

The phenomenon of deep holes occurs in all nuclei. However only in light nuclei does it touch the two adjacent upper shells—the filled and valence shells—and profoundly affects the structure of the GDR. It is precisely because of this phenomenon that transitions of type A and B in these nuclei are strongly separated in energy; a unified dipole state is not formed and the mechanisms of the GDR require a more detailed analysis. This situation was first pointed out in Ref. 20. We emphasize that at the time this was a new view of

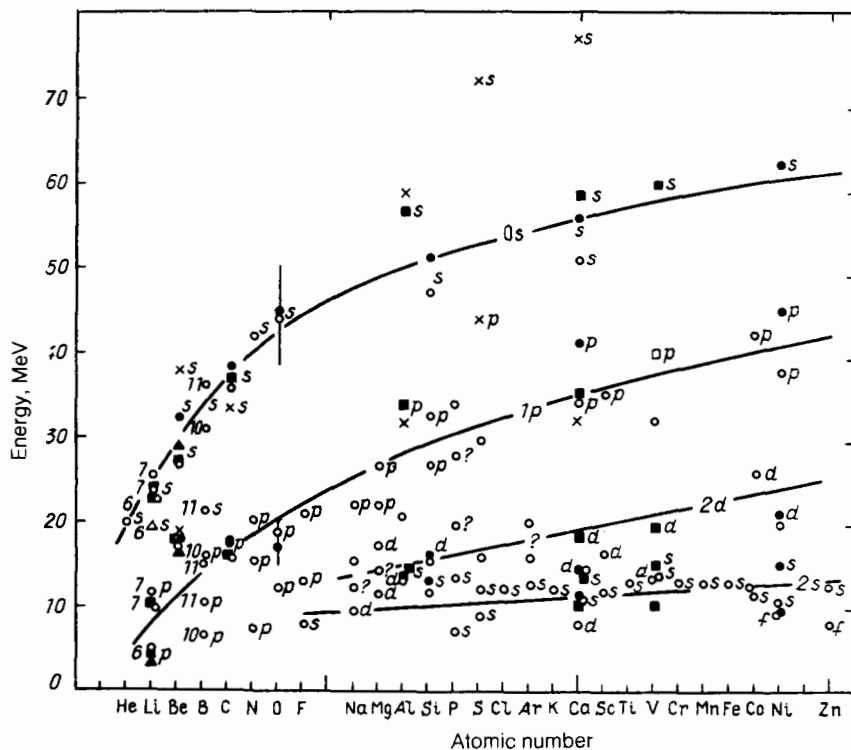


FIG. 4. The binding energies of protons in different shells, found from the reactions (e,e'p) (Ref. 9) and (p,2p) (Ref. 10).

the problem of GDR in light nuclei, since most specialists (and not only experimentalists) started from the hypothesis that in light nuclei the GDR is formed in a manner similar to the GDR in middle and heavy nuclei. Here the Fermi-gas model with pairing, which we mentioned earlier, in which the GDR depends only on the density of nuclear matter and the strength of the particle-hole interaction but not on the structure of the nuclei, had a "disciplining" effect.

We shall first see what the GDR in light nuclei would look like if deep holes were not fragmented and the residual interaction, mixing type A and B transitions, were not present. When the valence shell is first occupied, i.e., in nuclei of the type ${}^6,7\text{Li}$ and ${}^{17,18}\text{O}$, the valence nucleons form a pygmy resonance (this question is discussed in greater detail in Sec. 3), while the nucleons in the internal shells create the main branch in the transitions $0s \rightarrow 1p$ and $1p \rightarrow (2s, 2d)$. In this case, for example, in ${}^{18,17}\text{O}$ nuclei, the structure of the main branch of the GDR is close to that of the GDR in the ${}^{16}\text{O}$ nucleus. As the valence shell is filled the type A transitions become stronger while type B become weaker (because the number of vacant states in the valence shell decreases). In addition, the energy of type B transitions increases substantially (see the formula (34)). As a result in nuclei with an approximately half-filled shell the GDR will consist of two peaks separated significantly in energy and will look approximately like the picture shown in Fig. 5.

We shall now study more realistically the picture of configurational splitting of the GDR. For definiteness we shall have in mind 2s, 2d-shell nuclei; we shall study 1p-shell nuclei later. We shall first take into account the fact that strong spin-orbital splitting of the 1p-hole occurs: the $\overline{1p}_{3/2}$ state lies much higher than the $\overline{1p}_{1/2}$ state. This, generally speaking, should split the higher peak in Fig. 5 into two peaks. One of them (the one with the lower energy) will correspond to the type B transitions $1p_{1/2} \rightarrow 2s, 2d$ and the other will correspond to $1p_{3/2} \rightarrow 2s, 2d$. The peak corresponding to the $1p_{1/2} \rightarrow 2s, 2d$ transitions may occur in the region of the peak formed by type A transitions. The second significant factor is that the $1p_{3/2}$ -hole state is strongly fragmented, the fragmentation reaching, as we have already pointed out, 20 and more MeV. However, the $1p_{1/2}$ hole state is almost unfragmented. For example, in the ${}^{28}\text{Si}$ nucleus studied below all the spectroscopic strength of the proton

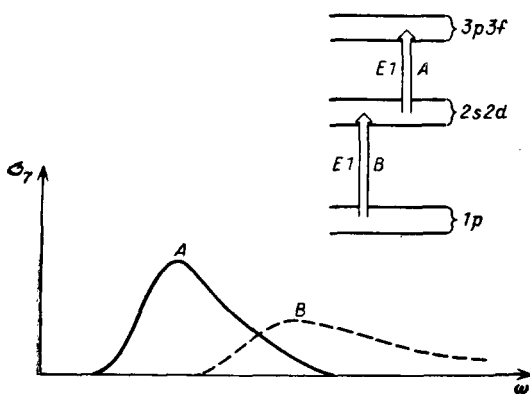


FIG. 5. The qualitative picture of the structure of the GDR in light 2s, 2d-shell nuclei assuming unfragmented hole levels.

$1p_{1/2}$ hole is concentrated in virtually one level of the ${}^{27}\text{Al}$ nucleus with an excitation energy of 4.05 MeV.

The strong fragmentation of the $1p_{3/2}$ hole will lead to two qualitative effects. First, in nuclei of the type ${}^{23}\text{Na}$, in which on the one hand the transitions $1p_{3/2} \rightarrow 2s, 2d$ play a very important role, while on the other the fragmentation of the hole has still not reached the limiting value of 20–30 MeV, the GDR is anomalously wide. In practice, in the ${}^{23}\text{Na}$ nucleus the GDR fills the entire energy band 18–30 MeV.

Second, in nuclei with very strong fragmentation of the $1p_{3/2}$ hole, for example, in the ${}^{28}\text{Si}$ nucleus and heavier nuclei, the transitions $1p_{3/2} \rightarrow (2s, 2d)$ should form a comparatively "limp" maximum with an area of 30–40% of the dipole sum rule at an energy of 25–30 MeV with a very long "tail" up to energies of 45–50 MeV. At the present time only the left edge of this peak has been observed. The group of type A transitions forms a distinct peak 5–7 MeV wide at an energy of ~ 20 MeV.

Finally, we shall discuss the role of the residual interaction. Since the transitions $1p_{1/2} \rightarrow 2s, 2d$ can lie in the region of the peak formed by type A transitions strong mixing of type A and $1p_{1/2} \rightarrow 2s, 2d$ transitions is possible. If, however, the energy of the transitions $1p_{1/2} \rightarrow 2s, 2d$ is several MeV higher than the type A resonance, the mixing will be insignificant. As an example Fig. 6 shows the results of calculations³⁷ of the GDR in the ${}^{32}\text{S}$ nucleus in the particle-hole and more complicated approximations. As one can see from the figure transitions of the type $1p_{1/2} \rightarrow 2s, 2d$ and $1p_{3/2} \rightarrow 2s, 2d$ remain independent.

Thus we can see that the formation of the GDR in light nuclei is determined by the aggregate effect of a number of factors, and the overall picture of the structure of the GDR can hardly be accurately calculated theoretically. For this reason it is especially important to confirm experimentally the main features of the semiquantitative picture presented above of the structure of the GDR.

The required experimental data, confirming the main features of the configuration splitting of the GDR in 2s, 2d-shell nuclei, were first obtained and analyzed by the photoneuclear group at the Scientific-Research Institute of Nuclear Physics at Moscow State University.^{38–40} The new progress made by this group reduces to the following. First, the group developed a method for measuring the partial cross sections of the (γ, p_i) reactions with a continuous (betatron) spectrum of γ rays. (Here the index i denotes the state of the final nucleus; zero corresponds to the ground state, one corresponds to the first excited state, etc.) Second, the partial cross sections of the (γ, p_i) reactions were measured for a wide set of 2s, 2d-shell nuclei right up to excitation energies of the final nuclei equal to 13 MeV (the endpoint energy E_γ^{\max} of the betatron spectrum was approximately 30 MeV). Third, it was shown, based on data on the proton pickup reactions of the type (n, d) and $(d, {}^3\text{He})$ and the reactions $(\gamma, p\gamma)$ and (γ, p_i) , that the decay of the GDR in light nuclei occurs, to a significant degree (50% and more), through the same configurations that are directly excited by the photons; in other words it was found that the semidirect effect reaches in like nuclei 50% and more of the total photoabsorption cross section. Fourth, by analyzing their data on partial cross sections and the published data on the total photoneuclear cross sections, this group was able to separate type A and B transitions and not only to establish the fact that con-

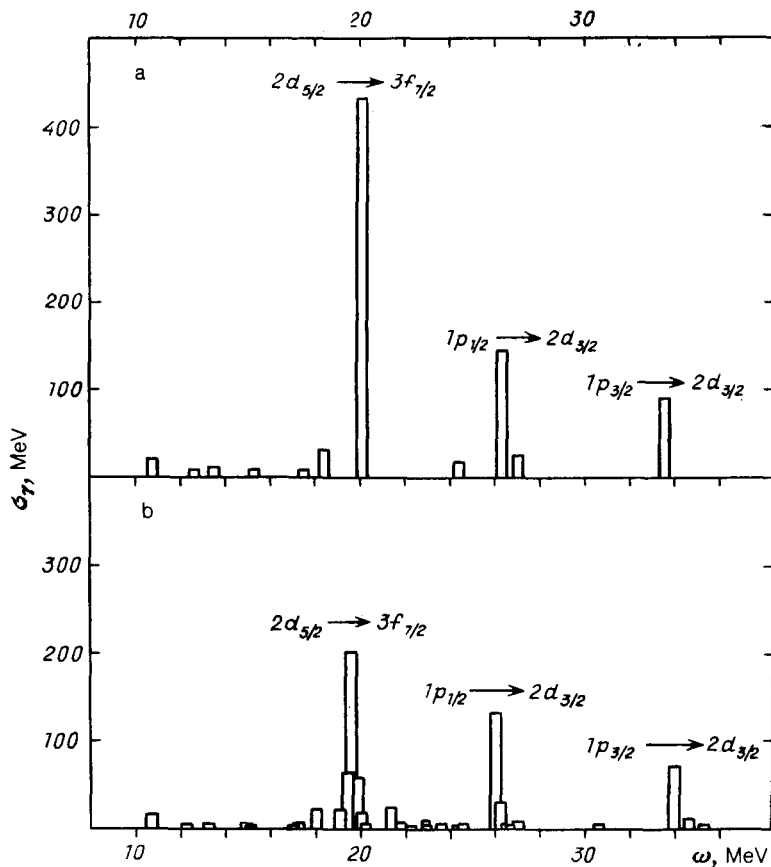


FIG. 6. The computed cross sections for the absorption of γ -quanta by the ^{32}S nucleus (Ref. 37) in the ph approximation (a) and taking into account more complicated configurations (b).

figurational splitting of the GDR occurs in 2s, 2d-shell nuclei, but also to observe a number of details and characteristic regularities of the GDR.

2.3. Experimental procedure for measuring the partial photonuclear cross sections with the betatron γ -ray spectrum

The essence of the method is explained in Fig. 7. The photonucleon spectra are measured in the γ -ray bremsstrahlung beam for different values of the endpoint E_γ^{\max} of the energy distribution of the γ -ray spectrum $W(\omega, E_\gamma^{\max})$. Each such spectrum is formed owing to decays of many states in the region of the giant resonance to different levels of the final nucleus $A-1$ and contains information about transitions into all occupied states. If the photonucleon spectra are measured with a small step of the endpoint E_γ^{\max} (a step ≈ 1 MeV is required), then the transitions into the state of the nucleus $A-1$ that have a different hole nature are separated. The main advantage of the method of extracting partial cross sections from photonucleon spectra lies in the possibility of obtaining the detailed energy dependence of the partial cross sections, which is a deciding factor in the observation and study of the configurational splitting of the dipole resonance.

The relation between the photonucleon spectra $N(\epsilon)$ and the partial photonucleon cross sections $\sigma_i(\omega)$ for the i th state of the final nucleus has the form

$$N(\epsilon) = \sum_i \sigma_i(\omega) W(\omega, E_\gamma^{\max}), \quad (36)$$

where ϵ is the kinetic energy of the nucleon, and ω, ϵ , and the

excitation energy of the final nucleus E_j are in their turn related by the relation

$$\omega = \frac{A}{A-1} \epsilon + B + E_i, \quad (37)$$

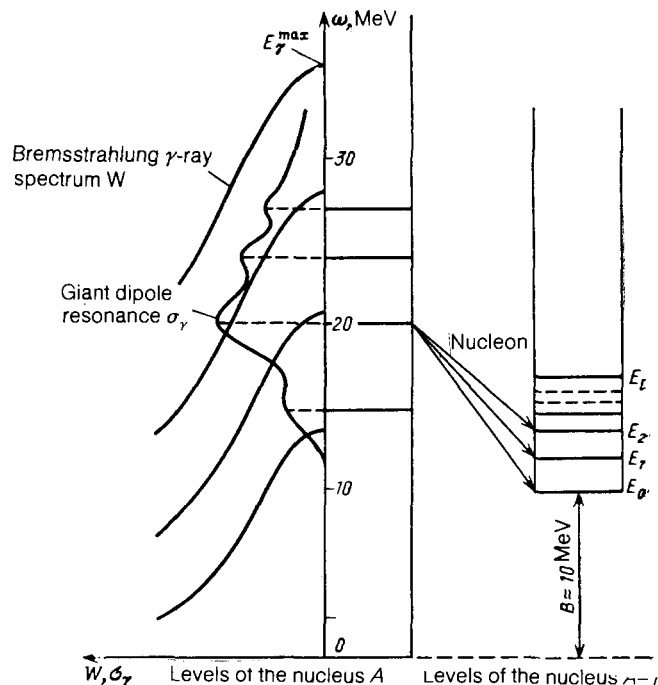


FIG. 7. The principle of the experiment on determining the energy dependences of the partial photonucleon cross sections in a bremsstrahlung beam.

where B is the separation energy of the nucleon.

The relations (36) for different values of E_{γ}^{\max} form a system of linear equations, by solving which one finds the partial cross sections $\sigma_i(\omega)$.

The experiment was performed in the bremsstrahlung beam of the betatron at the Scientific-Research Institute of Nuclear Physics at Moscow State University. Figure 8 shows a block diagram of the experiment. The photoproton reaction, which is the main reaction for most of the nuclei investigated, was studied. The beam of γ -quanta formed in the bremsstrahlung target placed inside the chamber of the betatron passed through a lead collimator 70 cm thick and entered the experimental chamber, separated from the accelerating chamber by a 2 m thick wall of lead and concrete. The target and the proton detectors were placed in a vacuum chamber. Measures were taken to improve as much as possible the background conditions of the experiment.

The operating regime of the accelerator and the apparatus employed to detect the charged particles were controlled by specially developed electronic devices. The system for stabilizing and varying the energy of the electrons in the betatron included the following: a unit for forming the tracking voltage, which is proportional to the instantaneous value of the intensity of the magnetic field $H(t)$ on an equilibrium orbit; a highly stable oscillator generating the stepped reference voltage; a circuit for comparing these quantities; and, a system for forming the pulse of accelerated electrons dumped onto the bremsstrahlung target. This system made it possible to maintain the energy of the accelerated electrons and therefore also E_{γ}^{\max} constant with an accuracy of 15-20 keV and to change this limit automatically according to a preselected program. To reduce the instantaneous load on

the detector and suppress the effects of repeated imposition of low-amplitude background pulses (from electrons and positrons) the duration of the γ -ray pulse was increased from 1 to 50 μsec . The processing and recording of information from the detectors were performed only during the γ -ray pulse. The energy of the betatron was calibrated based on the thresholds and well-known features in the yield curves of the photonuclear reactions. The value of E_{γ}^{\max} was determined with an absolute accuracy of about 100 keV.

The identification and detection of the protons together with a determination of their energies were performed with a telescope of semiconductor counters. The telescope made it possible to solve the problem of separating proton signals from the strong electron and positron background formed by nonnuclear processes and it allowed for detection of protons in the entire required range of energies (from 1.5 to 20 MeV). The energy resolution of the spectrometer was equal to 100-500 keV in the energy range 5-8 MeV. The nonlinearity of the spectrometric channel did not exceed 1%. The drift of the energy calibration of the spectrometer did not exceed 50 keV/day.

To obtain the partial cross sections $\sigma_i(\omega)$ from the photoproton spectra, measured for different values of E_{γ}^{\max} , these spectra had to be normalized with high accuracy. The problem of achieving the required accuracy in relative normalization was solved by using the principle of fast automatic variation (scanning) of the endpoint E_{γ}^{\max} of the bremsstrahlung beam. This methodological technique was first implemented in spectrometric photonuclear experiments. The following experimental regime was implemented: E_{γ}^{\max} was varied in each cycle of accelerator operation, i.e., with a frequency of 50 Hz, and made to pass successively and repea-

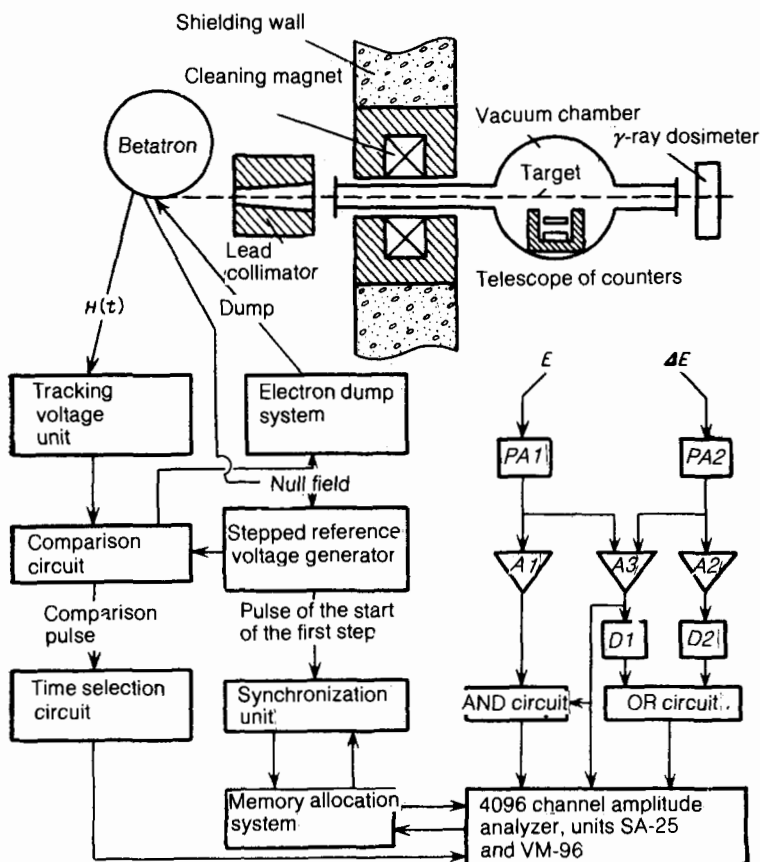


FIG. 8. Diagram of the experimental setup employed at the Scientific Research Institute of Nuclear Physics at Moscow State University for measuring the energy distributions of photoprotons under conditions of fast switching (scanning) of the endpoint of the bremsstrahlung spectrum. PA—preamplifier, A—amplifier, D—discriminator.

tedly through all planned values; the analyzer was changed synchronously and information on the energy distribution of the photoprotons was recorded on it. This operating regime, on the one hand, permits measuring simultaneously the photoproton spectra corresponding to different values of E_{γ}^{\max} , thereby suppressing the effect of long-time instability of the parameters of the spectrometric channel on the accuracy of the results; on the other, it completely removed the problem of protracted precision monitoring of the γ -ray dose, since at the end of the experiment all photonucleon spectra are automatically referenced to the same number of electron acceleration events.

Examples of the high efficiency and reliability of the experimental method developed as well as a more detailed description can be found in Refs. 41 and 42.

2.4. Configurational splitting of the GDR in 2s, 2d-shell nuclei. Experimental analysis

The starting point of the configuration analysis in light nuclei is the assumption that the semidirect effect plays the main role (50% and higher) in the decay properties of the GDR, i.e., the assumption that the decay of the GDR most likely occurs through a configuration directly excited through the absorption of γ -quanta. We stress that for heavy nuclei this assumption is definitely wrong: in heavy nuclei the GDR decays practically independently of its particle-hole structure.

A detailed discussion and comparison of extensive experimental data indicating that the analysis of the decay properties of the GDR, to a first approximation, can be confined to the semidirect photoeffect are contained in Ref. 3. For this reason we shall only give some illustrations. Figure 9 shows some data on the integrated cross section of the reactions (γ, p_0) (in units of $60 \text{ NZ/A MeV} \cdot \text{mb}$ —the values of the total integrated cross section based on the sum rule without the exchange term) and on the experimental spectroscopic factors,¹⁾ obtained from analysis of proton pickup reactions, for detachment of a 2s, 2d-proton from the target nucleus for a series of 2s, 2d-shell nuclei. As one can see from the figure there is a remarkable correlation between these two quantities, indicating that the reaction (γ, p_0) proceeds primarily by means of the semidirect mechanism and not by the statistical mechanism. The probabilities of occupation of different states of the final nucleus in the (γ, p) reaction with spectroscopic detachment factors of the proton from the nuclear target are compared in Fig. 10, also for a number of 2s, 2d-shell nuclei. The correlation between these quantities shows, also without any doubt, that the semidirect mechanism plays an important role in the decay of the GDR. Quantitative estimates of the contribution of the semidirect process for the ^{19}F nucleus are given in Ref. 45. According to these estimates, its contribution to the cross section of the (γ, p) reaction can reach 84%.

We shall study the main stages in the configurational analysis of the structure of the GDR for the example of the reaction (γ, p) on ^{28}Si nucleus. The partial cross sections of the reactions (γ, p_i) , in which groups of levels with the average energies $\bar{E}_i = 0, 0.9, 2.8, 4.0,$ and 6.4 MeV played the role of the i th level, were measured in Ref. 44. In reality each group of levels consisted of not more than two levels, well studied with the help of proton pickup reactions. The levels

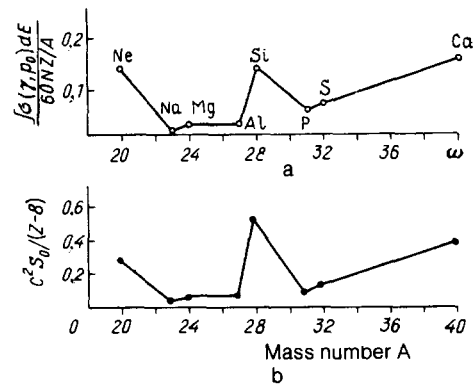


FIG. 9. Comparison of the integrated cross section of the reaction (γ, p_0) (a) with the spectroscopic factors for excitation of the ground state of the final nucleus in pickup reactions (b). The integral cross section is given in units of $60 \text{ NZ/A MeV} \cdot \text{mb}$ (the sum rule without the exchange term). The spectroscopic factor C^2S is normalized to the relative number of protons in the 2s, 2d shell.

entering into the first four groups have positive parity and practically exhaust the entire 2s, 2d-genealogy of the ^{28}Si nucleus. For this reason the total cross section for excitation of these levels should be given by, with good accuracy, the cross section for type A transitions. The 4.05 MeV level, contained in the next to last group, practically completely exhausts the $1p_{1/2}$ genealogy of the ^{28}Si nucleus. For this reason the probability of excitation of this level is determined by the cross section of $1p_{1/2} \rightarrow 2s, 2d$ -transitions. Finally, among the levels in the last group only one level is manifested in proton pickup reactions—the 5.16 MeV $3/2^-$ level.

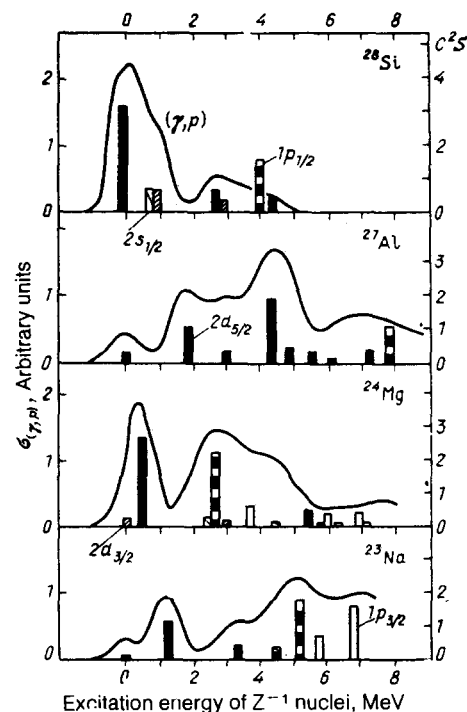


FIG. 10. Comparison of the distribution of the spectroscopic strength C^2S of single-particle levels with occupation probabilities of different levels of the final nucleus in the reaction (γ, p) . The target nuclei are indicated in the upper righthand corner.

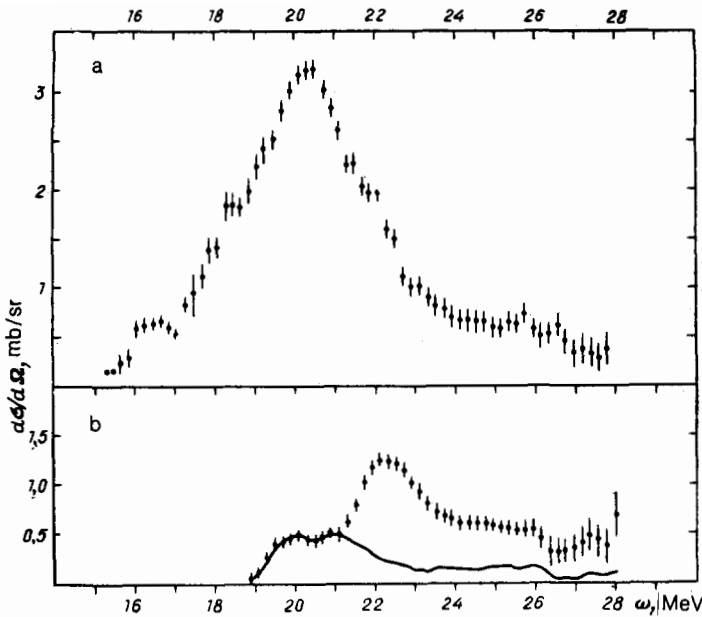


FIG. 11. Cross sections of type A and B transitions (Figs. a and b, respectively) in the ^{28}Si nucleus.⁴⁴ The solid curve in Fig. b is the cross section of $1p_{1/2} \rightarrow 2s, 2d$ transitions.

It exhausts about 30% of the spectroscopic strength of the $1p_{3/2}$ hole. For this reason it is natural to interpret the cross section for the excitation of the last group ($E_i = 6.4$ MeV) as the cross section of $1p_{3/2} \rightarrow 2s, 2d$ -transitions. The result of this analysis is shown in Fig. 11. If published data on the total photonuclear cross section on the ^{28}Si nucleus are employed and the difference between this cross section and the cross section for the excitation of levels exhausting the $2s, 2d$ -genealogy of the ^{28}Si nucleus is interpreted as the cross section of type B transitions, then we obtain the picture shown in Fig. 13a. A like analysis was performed for a number of other $2s, 2d$ -shell nuclei. The result of this analysis is shown in Figs. 12 and 13.

We shall now discuss the main features of the configurational splitting of the GDR in $2s, 2d$ -shell nuclei. Probably the most important conclusion that can be drawn from Figs. 12 and 13 is that the transitions $2s, 2d \rightarrow 3p, 3f$ and $1p_{1/2} \rightarrow 2s, 2d$ die out by $\omega = 30$ MeV, while the intensity of the transitions $1p_{3/2} \rightarrow 2s, d$, on the contrary, are at full strength at 30 MeV. For this reason it is natural to assume that the "tail" of the GDR is determined precisely by these transitions. The most important problem is to confirm this very important assertion experimentally (the endpoint of the spectrum of the betatron at the Scientific-Research Institute of Physics at Moscow State University did not exceed 30 MeV).

The energy "centers of gravity" \bar{E} of type A transitions and the transitions $1p_{1/2} \rightarrow 2s, 2d$, defined as

$$\bar{E} = \int_{E_{th}}^{30} \sigma(\omega) \omega d\omega \left(\int_{E_{th}}^{30} \sigma(\omega) d\omega \right)^{-1}, \quad (38)$$

differ by approximately by 2 MeV (Table I). This fact can be interpreted as indicating that the type A transitions do not mix with the transitions $1p_{1/2} \rightarrow 2s, 2d$, i.e., a single dipole state is not formed even from type A and $1p_{1/2} \rightarrow 2s, 2d$ -transitions.

The special properties of $1p_{3/2} \rightarrow 2s, 2d$ transitions—the increasing fragmentation of the $1p_{3/2}$ hole—are the only basis, it seems to us, for understanding the unusual extended

GDR in the ^{23}Na nucleus (see Figs. 12 and 13). Finally, Fig. 14 shows the experimentally determined probabilities of A-transitions for a number of $2s, 2d$ -shell nuclei.

Thus far we have relied on the data from Refs. 38–40 obtained by the photonuclear group at the Scientific-Research Institute of Physics at Moscow State University. Over the last few years the configurational splitting in $2s, 2d$ -shell nuclei has been studied by other photonuclear groups also. Here we confine ourselves to a brief discussion of the results obtained in the excellent work of Ref. 45, which is devoted to the (γ, p_i) reaction on the ^{19}F nucleus. The authors of this work were able to measure the cross section of (γ, p_i) reactions on ^{19}F for seven groups of levels of the final nucleus ^{18}O . Relying on the spectroscopic data on the proton pickup reaction, they were able to separate type A and B transitions, just as the group at Moscow State University was able to do earlier. Figure 15 shows their measurements of the cross sections of (γ, p_i) reactions, and Table II gives the characteristics and spectroscopic factors of the excited groups of levels of the final ^{18}O nucleus. The γ -ray absorption cross section of the ^{19}F nucleus, which they found from a general analysis, is presented in Fig. 16. As one can see from Figs. 16 and 15 and Table II two overlapping maxima clearly come through in the absorption cross section—one near 20 MeV and the

TABLE I. The centers of gravity \bar{E} of the cross sections for the transitions $1p_{1/2} \rightarrow 2s, 2d$ and $2s, 2d \rightarrow 3p, 3f$ and their difference $\Delta\bar{E}$ (estimates for $\omega \leq 30$ MeV).

Nucleus	$2s, 2d \rightarrow 3p, 3f$ \bar{E}, MeV	$1p_{1/2} \rightarrow 2s, 2d$ \bar{E}, MeV	$\Delta\bar{E}, \text{MeV}$
^{23}Na	20.1	22.0	1.9
^{24}Mg	21.6	22.8	1.2
^{25}Mg	21.3	22.7	1.4
^{26}Mg	22.1	23–24	1–2
^{27}Al	20.4	23.2	2.8
^{28}Si	20.9	22.2	1.3
^{31}P	21–22	25	3–4
^{32}S	20.4	21.9	1.5
^{40}Ca	20–21	25	4–5

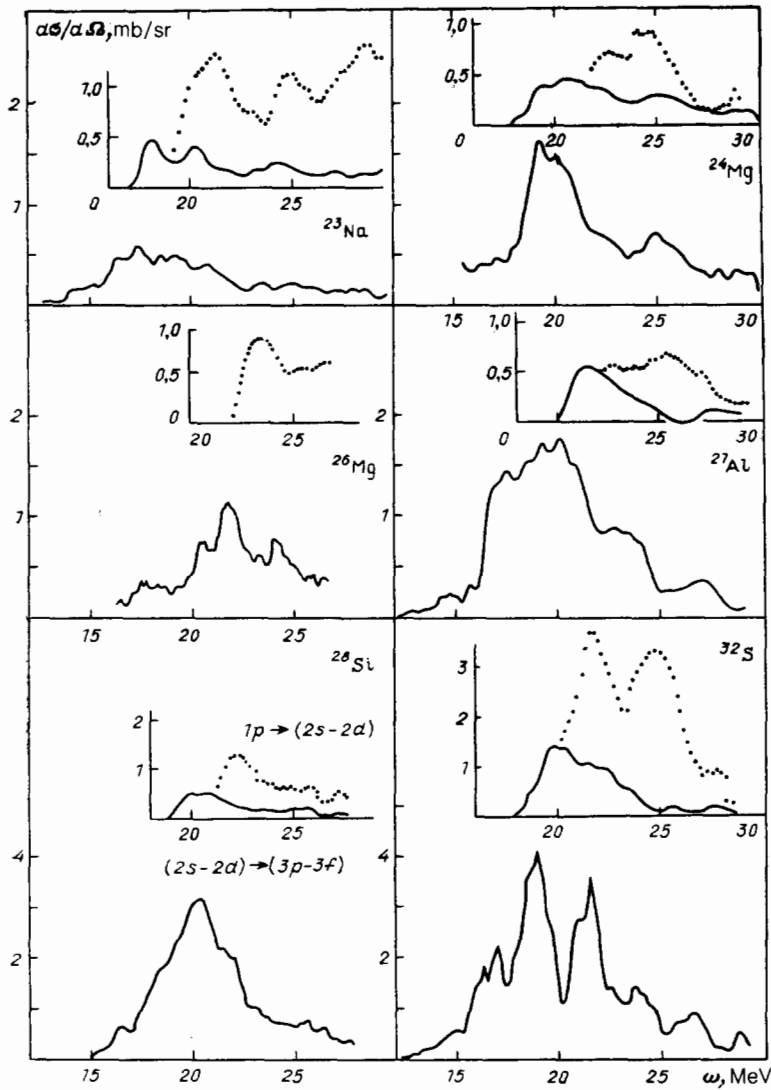


FIG. 12. Separation of the total photoproton cross sections for the nuclei ^{23}Na , ^{24}Mg , ^{26}Mg , ^{27}Al , ^{28}Si and ^{32}S into cross sections of type A and B transitions.⁴² The cross section of the $1p_{1/2} \rightarrow 2s$, $2d$ and $1p \rightarrow 2s$, $2d$ transitions are shown in the insets by the solid and dotted lines, respectively.

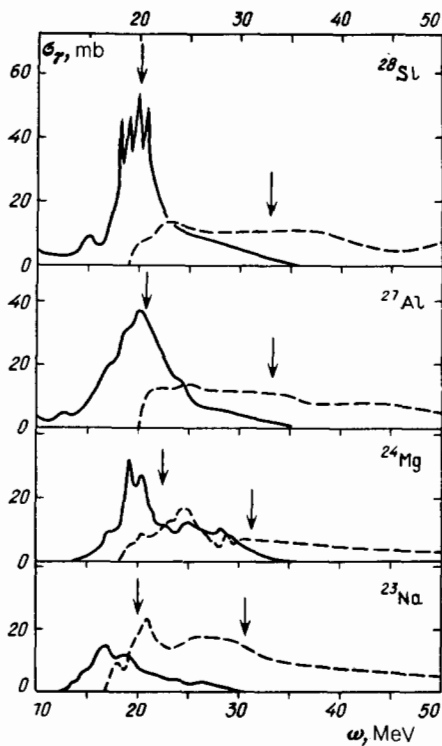


FIG. 13. The photoabsorption cross section of ^{28}Si , ^{27}Al , ^{24}Mg and ^{23}Na nuclei at energies up to 50 MeV, divided into type A (solid curves) and type B (broken curves) transitions.³⁹

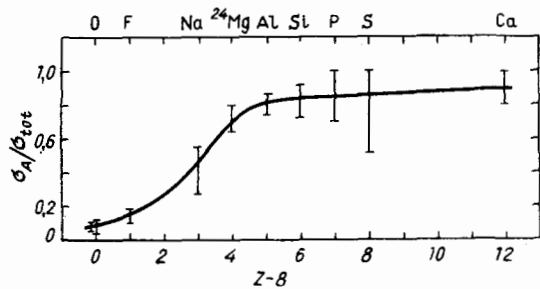


FIG. 14. The relative fraction (σ_A/σ_t) of the cross section of type A transitions as a function of the total absorption cross section for γ -quanta in 2s, 2d-shell nuclei; Z is the charge of the nucleus.

other near 25 MeV. In addition, the intensity of type A transitions practically drops to zero by $\omega = 25$ MeV. Thus the second maximum must be interpreted as being due to type B transitions, i.e., $1p \rightarrow 2s, 2d$ transitions. Therefore the configurational splitting, i.e., the shift in the energies of 2s, 2d $\rightarrow 3p3f$ and $1p \rightarrow 2s, 2d$ transitions, is equal to 5 MeV.

In concluding this section we shall discuss several questions which are primarily of historical interest. The concept of configurational splitting in 2s, 2d-shell nuclei was first stated in 1964.²⁰ Since then indirect data on configurational splitting has accumulated steadily. They include the following.

a) The region of absorption of γ -quanta in the ^{24}Mg nucleus is appreciably larger than indicated by theoretical calculations based on the generalized model in Ref. 46.

b) The curve of the cross section of elastic scattering of γ -quanta by ^{24}Mg , ^{27}Al , ^{28}Si , and ^{32}S nuclei has two humps.²⁴ As an example, Fig. 17 shows the experimental curve of the elastic scattering of γ rays by the ^{32}S nucleus together with the computational results of Ref. 37. The significant suppression of the nucleon channel in type B transitions (owing to the decrease in the energy of the nucleons) leads to a second peak in the elastic channel in the region where they are concentrated.

c) Two absorption bands were discovered in (γ, n) reactions²⁴ on ^{19}F , ^{20}N , and ^{23}Na nuclei; one ($\omega = 22\text{--}26$) is the analog of the GDR in the ^{16}O nucleus. In addition, the absorption cross section in the high-energy band decreases as A increases, while the absorption cross section in the low-

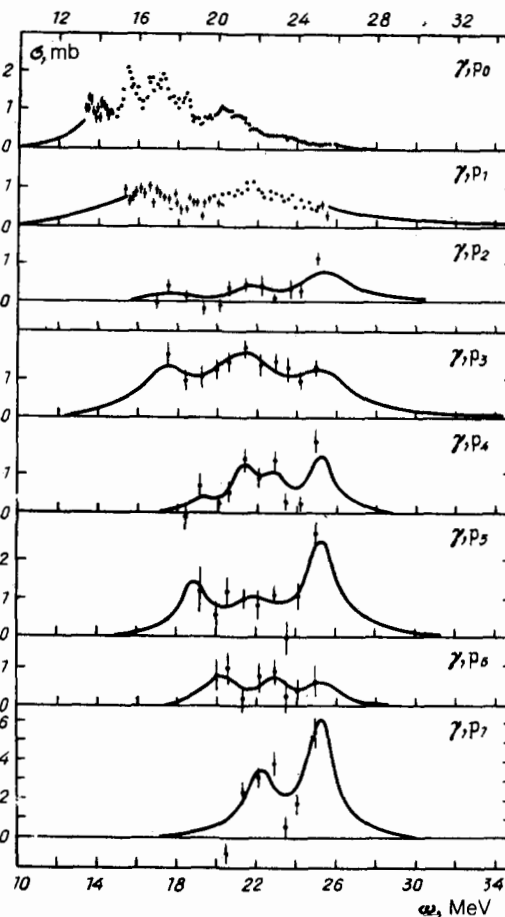


FIG. 15. The partial cross sections of the reactions (γ, p_i) on the $^{19}\text{F}^{45}$ nucleus. The solid curves are shown in order to visualize the information.

energy region ($\omega = 18\text{--}21$ MeV) increases. The authors of these studies stated the hypothesis that the lefthand peak is due to type A transitions and the righthand peak is due to type B transitions. It is instructive to note that in experiments of the type $(\gamma, p_0 + p_1)$, which have dominated for many years, the righthand side of the GDR in light nuclei, appearing as a result of type B transitions, could not be observed at all. This is connected with one of the most important aspects of configurational splitting—the absence of full

TABLE II. The integrated cross sections of the reactions $^{19}\text{F}(\gamma, p_i)^{18}\text{O}$ and the characteristics of the occupied states of the final nucleus.

The index i of the partial cross section	E_i , MeV	The hole configuration nlj	Spectroscopic factor C^2S	The integrated cross section, MeV·mb
0	0	$2s_{1/2}$	0.38	8.7
1	1.98	$2d_{5/2}$	0.53	9.5
2	3.63	$4d_{5/2}$	0.04	2.3
		$2s_{1/2}$	0.05	
3	4.45	$2d_{5/2}$	0.02	13.4
		$1p_{1/2}$	1.31	
4	5.28	$2d_{5/2}$	0.32	5.7
		$2s_{1/2}$	0.15	
5	6.27	$1p_{3/2}$	0.70	7.6
6	6.88	$1p_{1/2}$	1.03	2.5
7	7.67	$1p_{3/2}$	0.42	13.6

For $i = 2, 4, 5, 6$, and 7 the partial cross sections are the cross sections for the occupation of groups of states of the final nucleus.

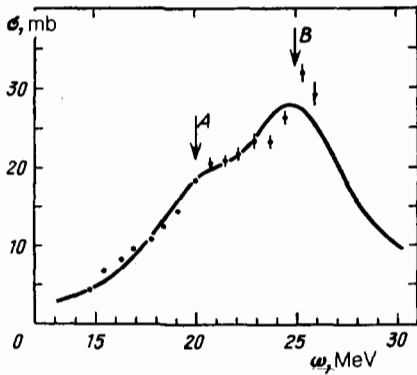


FIG. 16. The total γ -quantum absorption cross section of the ^{19}F nucleus.⁴⁵ The solid line is the sum of the Lorentz curves corresponding to type A and B transitions.

collectivization of ph configurations. The need for measuring the cross sections of (γ, p_i) channels with sufficiently high excitation of the final nuclei was acknowledged and the existence of configurational splitting was unambiguously proved only in Refs. 38–40 at the end of the 1970s and the beginning of the 1980s (see also Ref. 47).

2.5. Deep holes and the structure of the GDR in 1p-shell nuclei

We shall now study the features of the configurational splitting of the GDR in 1p-shell nuclei which are determined by the existence of a deep hole. Type A and B transitions have not yet been separated experimentally in these nuclei. For this reason we based our analysis of the role of a deep 0s-hole on the theoretical calculations of the GDR in these nuclei, performed by the BSM($1\hbar\omega$) method in Ref. 47. Figure 18 shows the computed total cross sections of the GDR in the nuclei ^7Li , ^9Be , ^{11}B , $^{13-15}\text{C}$, and $^{14,15}\text{N}$. The line cutting across the figure separates type A and B transitions: absorption to the right of the line is determined by type B transitions.

Analyzing this figure we note first of all that type A and B transitions in 1p-shell nuclei mix insignificantly and a single dipole state is not formed. The structure of the A branch of the GDR depends very strongly on the supermultiplet nature of the splitting and will be studied in the next section. Transitions of type B, as one would expect, are most important in nuclei in which the 1p-shell is just starting to be occupied, i.e., in ^7Li and ^9Be nuclei. Calculations by the BSM($1\hbar\omega$) method describe qualitatively correctly the

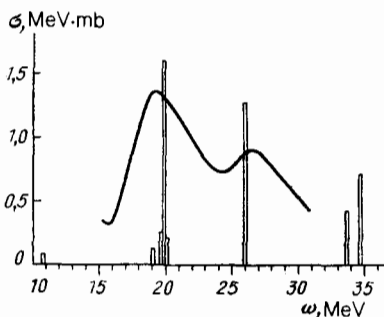


FIG. 17. The computed (columns) and measured cross sections of the (γ, γ_0) reaction on the ^{32}S nucleus.³⁷

main feature of the GDR in these nuclei—the fact that it is strongly extended (Fig. 19). For example, in ^9Be the GDR extends up to 50 MeV. However the GDR in these nuclei is not reproduced very well quantitatively. This deficiency of the theory is most likely connected with the inadequate treatment given in Ref. 47 of the fragmentation of the 0s hole. The intensity of type A and B transitions are the same in ^9Be nucleus, and in heavier nuclei type B transitions play a subordinate, somewhat exotic role, forming the 30-MeV and higher energy region of the GDR.

In conclusion we shall briefly discuss the question of deep holes in heavier nuclei, more specifically, 3p, 3f-shell nuclei. Estimates of ε from the formula (34) for 3p, 3f-shell nuclei give⁴⁸

$$\varepsilon_{3p, 3f} \approx 0,6-0,8 \text{ MeV.} \quad (35')$$

For this reason appreciable broadening of the GDR can be expected in 3p, 3f-shell nuclei with $N-20 \approx 10$ or $Z-20 \approx 10$. This question, however, has not yet been completely resolved.

3. GDR AND THE SUPERMULTIPLY STRUCTURE OF 1p-SHELL NUCLEI

3.1. Supermultiplet symmetry

The structure of the A branch of the GDR in 1p-shell nuclei depends very strongly on the supermultiplet symmetry, i.e., the SU_5 spin-isospin group of 1p-shell nuclei. We shall study first some general manifestations of the supermultiplet symmetry. It is well known⁴⁹ that the irreducible representations and therefore the multiplets of the SU_4 group are in general given by Young's schemes $[f] = [f_1, f_2, f_3, f_4]$ with $f_1 \geq f_2 \geq f_3 \geq f_4$ and $\sum f_i = A$, where A is the number of nucleons in the nucleus. Because the wave function of the nucleus is antisymmetric the SU_4 supermultiplets can also be specified with the help of Young's scheme for the permutational symmetry of the spatial part of the wave function. This scheme, which we shall also denote by the index $[f]$, is the conjugate Young scheme of the SU_4 group and is specified by the collection of numbers $[f] = [f_1, f_2, \dots, f_n]$ with $f_1 \geq f_2 \geq \dots \geq f_n$, $f_i < 4$ and $\sum f_i = A$. It is precisely in these terms that we shall discuss below the structure of 1p-shell nuclei.

The effects of supermultiplet symmetry—supermultiplet splitting of the levels of light nuclei—arise owing to the distinguished role of Majorana's forces, i.e., pair forces of the type

$$\hat{V}_{12} = -V(r) \hat{P}_{12}^X, \quad (39)$$

where \hat{P}_{12}^X is Majorana's operator—the operator permuting the spatial coordinates of the nucleons—and $V(r)$ is a radial function that specifies the strength of the interaction and its radial dependence.

We shall assume first that the energies of the states can be evaluated in the approximation “diagonal” with respect to the configurations, i.e., as the average values of the Hamiltonian (24) over fixed shell configurations. Denoting by \bar{V} the average strength of the pair interaction in a given configuration we obtain for the operator \hat{M} of the total Majorana interaction

$$\hat{M} = -\bar{V} \sum_{\langle ij \rangle} \hat{P}_{ij}^X. \quad (40)$$

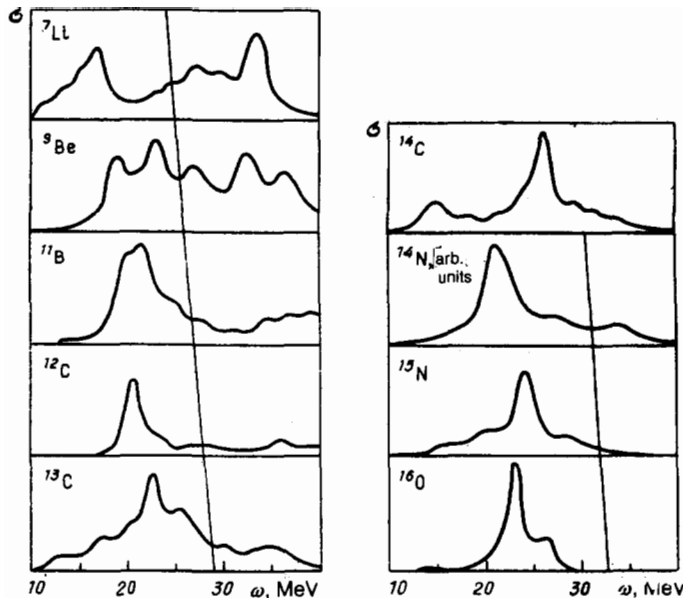


FIG. 18. The computed γ -quantum absorption cross sections of 1p-shell nuclei.⁴⁷ The columns obtained in the calculations are "broadened" using the Wigner-Breit formula with a width $\Gamma = 2$ MeV. The solid secant line separates type A transitions (on the left) from type B transitions (on the right).

It is easy to see that the operator $\sum_{i < j} \hat{P}_{ij}^x$ is an invariant of the permutation group of the spatial coordinates of the nucleons (more precisely, the Casimir operator of this group). The eigenvalues of this operator for the representation (of the supermultiplet) $[f]$ are given by the formula

$$\langle [f] | \sum_{i < j} \hat{P}_{ij}^x | [f] \rangle = \frac{1}{2} [f_1(f_1 - 1) + f_3(f_3 - 3) + \dots]. \quad (41)$$

It follows from here that the states belonging to different Young schemes must be separated by a large energy interval. We shall illustrate this for the example of ${}^6\text{Li}$ and ${}^7\text{Li}$ nuclei. Shell calculations⁵⁰ show that in ${}^6\text{Li}$ the states with the

Young scheme [42] and the configuration $0s^4 1p^2$ and in ${}^7\text{Li}$ the states with the scheme [43] and the configuration $1s^4 1p^3$ lie in the energy interval 0–6 MeV (the energy is measured from the ground state). The states in ${}^6\text{Li}$ and ${}^7\text{Li}$ with the Young schemes [411] and [421] lie in the range 10–20 MeV! An analogous situation also occurs in other 1p-shell nuclei.

The strongest and most stable effects of supermultiplet splitting arise with changes in the Young scheme such that the number of "fours" in them decreases. Phenomena associated with the change in the number of "fours" in Young's scheme are called "fouring" effects.²⁰ We shall illustrate the existence of this effect for the example of the nuclei ${}^8\text{Be}$ and ${}^{12}\text{C}$. The ground state of these nuclei correspond to the Young schemes [44] and [444]. The isospin of these states should be zero (all nucleons are combined into groups of four). The states arising when the combinations of four are broken up, i.e., states with the Young schemes [431] and [4431], can have the isospin $T = 1$ and, as spectroscopy shows, they are found at energies $E \geq 15$ –16 MeV. The number 15–16 MeV is the characteristic energy of formation of groups of four nucleons in all 1p-shell nuclei.

3.2. Effects of supermultiplet symmetry in the GDR

We shall now trace the manifestations of the effects of supermultiplet splitting in the GDR. We start once again from the lightest 1p-shell nuclei— ${}^6\text{Li}$ and ${}^7\text{Li}$. In these nuclei the GDR is formed by the following configurations:

$$\begin{aligned} {}^6\text{Li}: & \quad 0s^4 1p(2s, 2d) [411], \\ & \quad 0s^3 1p^2 [33], \\ & \quad 0s^3 1p^3 [321], \end{aligned} \quad (42)$$

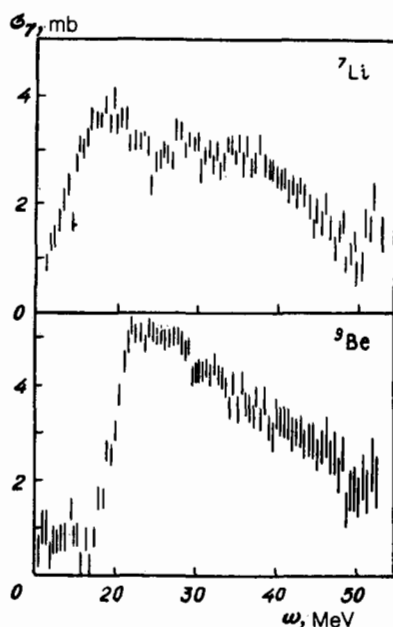


FIG. 19. The measured γ -quantum absorption cross sections of ${}^7\text{Li}$ and ${}^9\text{Be}$ nuclei.⁶²

TABLE III.

Energy range, MeV	Young's schemes of the excited configurations
10–15	[411], [43]
15–20	[33], [421]
25–35	[321], [331]

$$\begin{aligned}
{}^7\text{Li}: & \quad 0s^4 1p^2 (2s, 2d) \quad [43], [421], \\
& \quad 0s^3 1p^4 \quad [43], \\
& \quad 0s^3 1p^4 [331].
\end{aligned} \tag{43}$$

According to Sec. 3.1 the energies of the configurations $0s^3 1p^3$ [33] in ${}^6\text{Li}$ and $0s^3 1p^4$ [331] in ${}^7\text{Li}$ must be significantly (≈ 10 MeV)⁽²⁾ greater than the energies of the configurations $0s^4 1p(2s, 2d)$ [411], $0s^4 1p^2(2s, 2d)$ [43], [421] and $0s^3 1p^4$ [43]. Some of the additional spread in the configuration energies for ${}^6\text{Li}$ is related with the fact that two Young schemes are operating—[321] and [33]. As a result one would expect that the absorption of γ quanta in the isotopes of Li should be concentrated in the energy ranges given in Table III.

Since the decay properties of the GDR in light nuclei are largely determined by the configurations directly excited by γ -quanta the rules for multiplying Young schemes⁴⁹ dictate the preferred types of decays of GDR in lithium isotopes:

$$\begin{aligned}
0s^4 1p(2s, 2d) [411] & \rightarrow \alpha + p + n, \\
0s^3 1p^3 [33] & \rightarrow t + {}^3\text{He}, \\
0s^3 1p^3 [321] & \rightarrow \begin{cases} t + d + p, \\ {}^3\text{He} + d + n, \end{cases} \\
0s^3 1p^4, 0s^4 1p^2(2s, 2d) [43] & \rightarrow \alpha + t, \downarrow \\
0s^4 1p^2(2s, 2d) [421] & \rightarrow \begin{cases} {}^5\text{He} + d \rightarrow \alpha + d + n, \\ {}^6\text{Li}^* [42] + n \begin{cases} \rightarrow {}^6\text{Li} + n + \gamma, \\ \rightarrow \alpha + d + n, \end{cases} \end{cases} \\
0s^3 1p^4 [331] & \rightarrow \begin{cases} t + t + p, \\ t + {}^3\text{He} + n. \end{cases}
\end{aligned} \tag{44}$$

For greater clarity the types of decay of the ${}^6\text{Li}$ nucleus are shown in Fig. 20. The most remarkable property of GDR in ${}^6,7\text{Li}$ nuclei must be the high probability of decay in the channels α -t and ${}^3\text{He}$ -t and the "star" channel, i.e., multiparticle channels corresponding to different parts of the dipole absorption band. Analysis of the experimental data (the details are given in Ref. 43) on the whole confirms this theory, but the theory does not always agree quantitatively with experiment. Evidently still more experimental and theoretical work must be done in order to understand on a quantitative

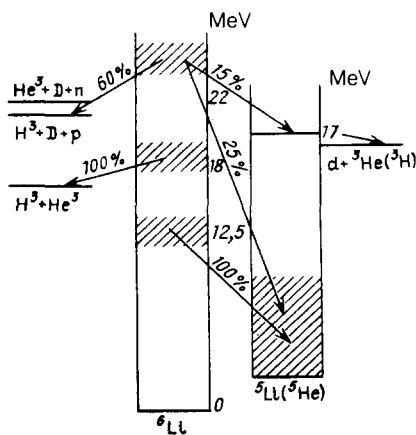


FIG. 20. Diagram of excitation of ${}^6\text{Li}$ nuclei by γ -quanta and subsequent decay, predicted by the theory in the "diagonal" approximation.

level the details of the photosplitting of Li isotopes. In particular, definite deviations from the shell factors toward the α -particle mechanism of γ -ray absorption are possible.⁵¹

A good test of the theory studied here could be the photosplitting of the ${}^9\text{Be}$ nucleus. The configuration of the ground state of this nucleus is $0s^4 1p^5$ [441]. In type A transitions the configurations $0s^4 1p^4(2s, 2d)$ with the Young schemes [441], [432], and [4311] are excited. According to what was said above, states with the Young schemes [441], [432], and [4311] are separated by an energy interval equal to approximately 15–16 MeV (the "fouring" effect). Correspondingly the set of states with the Young schemes [432] and [4311] forms the principal peak of the GDR in ${}^9\text{Be}$, lying in the region 15–25 MeV, while states with Young scheme [441] give the pygmy resonance, which is clearly seen in the (γ, n) channel (Fig. 21). The pygmy resonance, naturally, should lie at significantly lower energies.

The decay properties of the GDR in ${}^9\text{Be}$ are also representative. In the final nucleus ${}^8\text{Be}$ states with the Young scheme [44] occupy the interval 0–15 MeV (in all such levels the isospin is equal to zero). The first level with the isospin $T = 1$ and correspondingly with the Young scheme [431] appears at 15 MeV. From here it follows that decays of the principal peak of the GDR in ${}^9\text{Be}$ to low-lying states of ${}^8\text{Be}$ are also forbidden by the selection rules according to Young's schemes: by removing one nucleon it is impossible to obtain from the Young schemes [432] and [4311] the scheme [44]. We encounter here the general property of the GDR in 1p-shell nuclei—in these nuclei the GDR decays predominantly into highly excited states of the final nuclei. Conversely, the pygmy resonance, which is characterized by the Young scheme [441], can decay into low-lying states (in particular, the ground state) of the final nucleus. It is for this reason that it is observed in the neutron channel.

The supermultiplet properties of the ${}^{13}\text{C}$ nucleus are very close to those of the ${}^9\text{Be}$ nucleus. Everything that has been said for ${}^9\text{Be}$ is also true for ${}^{13}\text{C}$. The only change that must be made, formally, is that the Young schemes must be changed: [441] \rightarrow [4441], etc.

For this reason, the ${}^{13}\text{C}$ nucleus should have a pygmy resonance just like the ${}^9\text{Be}$ nucleus. It can easily be seen experimentally (once again in the (γ, n) channel). The nuclei ${}^{11}\text{B}$, ${}^{14}\text{C}$, and ${}^{15}\text{N}$, which have nucleons which are not "foured" (see Ref. 43 for a detailed discussion), also have a pygmy resonance. The ${}^{14}\text{N}$ nucleus could also have a pygmy

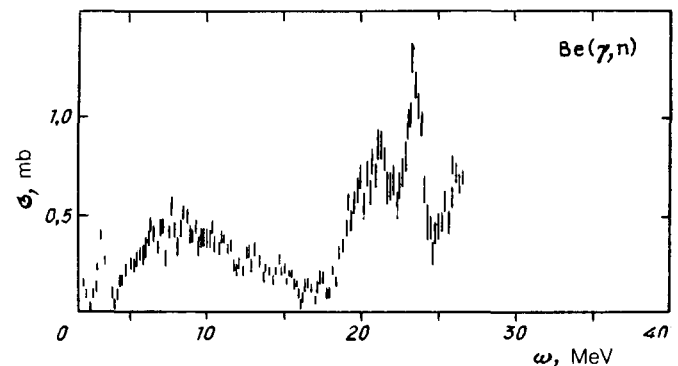


FIG. 21. The cross section of the ${}^9\text{Be}(\gamma, n)$ reaction measured by Hughes *et al.*⁴⁷

TABLE IV. The weights of the dominant components in the wave function of the ground state of 1p-shell nuclei and in the LS representation (variant of the Hamiltonian with Rosenfeld's forces).

Nucleus	Main component [f] ^{2T+1 2S+1 L_J}	Wt. %	Nucleus	Main component [f] ^{2T+1 2S+1 L_J}	Wt. %
⁷ Li	[3] ²² P _{3/2}	97	¹² C	[44] ¹¹ S ₀	71
⁸ Be	[4] ¹¹ S ₀	97	¹³ C	[441] ²² P _{1/2}	84
⁹ Be	[41] ²² P _{3/2}	81	¹⁴ N	[442] ¹² D ₁	90
¹⁰ B	[42] ¹² D ₃	64	¹⁴ C	[442] ²¹ S ₀	56
¹¹ B	[43] ²² P _{3/2}	41	¹⁵ N	[433] ²² P ₀	44
	[43] ²² D _{3/2}	32		[443] ²² P _{1/2}	100

resonance, but because in this nucleus the "fouring" effect is significantly weaker than in the neighboring odd nuclei, the residual interaction mixes the configurations in a manner so as to form a single wide absorption maximum.

Thus far we have neglected the residual interaction and studied the supermultiplet properties of the GDR in the diagonal approximation. Of course, the residual, with respect to this diagonal approximation, interaction will destroy to a certain extent the supermultiplet structure of the nuclear states. However numerous calculations of the GDR in 1p-shell nuclei in the BSM(1 $\hbar\omega$) approximation showed that the supermultiplet gross structure of the GDR is nonetheless preserved. Table IV gives the weights of the dominant components of the wave functions of the ground states of 1p-shell nuclei. It is evident from this table that for the ground states of 1p-shell nuclei one can talk with reasonable accuracy about the manifestation of a supermultiplet structure. The supermultiplet composition of the excited states forming the GDR was not specially studied. However indirect data leave no doubt about the gross supermultiplet structure of the GDR in 1p-shell nuclei. We shall confine ourselves here to only one argument, based on comparing the GDR in the nuclei ⁷Li and ⁹Be. In ⁷Li the peak near 15 MeV is due to 1p→2d transitions. In ⁹Be, however, the peak associated with 1p→2d transitions lies in the region 20–25 MeV. The most natural explanation of this phenomenon reduces to the following. In ⁹Be the 1p-shell contains (in contradistinction to ⁷Li) "foured" nucleons. The main peak of the 1p→2d transitions is associated with the destruction of a "four" and therefore its energy is strongly shifted upwards.

In conclusion we note that the supermultiplet effects of the GDR are substantially weaker in 2s, 2d-shell nuclei, and they no longer can be clearly distinguished, irrespective of the diagonalization of the Hamiltonian (24). This is associated both with the increased role of the spin-orbital interaction and the decrease in the strength of the monopole part of the Majorana forces.

4. THE UNIVERSALITY OF THE CONFIGURATIONAL SPLITTING PHENOMENON

The phenomenon of configurational splitting of the GDR studied in the preceding sections is caused, as we saw, by the nontrivial characteristics of the Hartree-Fock shell potential—the sharp drop of the deep shell levels (the phenomenon of deep holes) and the supermultiplet symmetry of light nuclei. It is easy to see, however, that the configurational splitting, understood as the characteristic structure of the

excitation spectrum of a light nucleus, must be manifested not only under the action of the electric dipole field of a γ quantum on the nucleus, but also under the action of the spin-isospin dipole field on it. The dipole and spin-dipole external fields effectively arise in the processes

$$\mu^- + (A, Z) \rightarrow \nu_\mu + (A, Z-1), \quad (45)$$

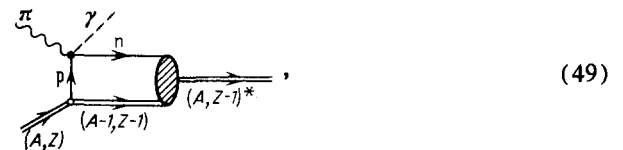
$$\pi^- + (A, Z) \rightarrow \gamma + (A, Z-1), \quad (46)$$

$$\gamma + (A, Z) \rightarrow \pi^+ + (A, Z-1), \quad (47)$$

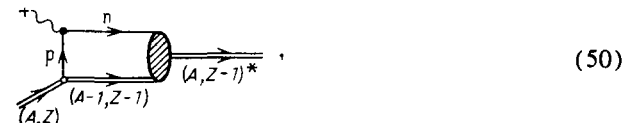
$$n + (A, Z) \rightarrow p + (A, Z-1) \quad \text{etc.}, \quad (48)$$

where (A, Z) denotes an atomic nucleus with mass number A and charge Z; μ^- , π^\pm , γ , and ν_μ are muons, pions, γ quanta, and the muon neutrino. Referring the interested reader to the monographs and reviews of Refs. 52–58, we confine ourselves here to a qualitative analysis of these reactions and examples.

It turns out that to a first approximation the reactions (45)–(48) can be described in the impulse approximation, i.e., with the help (for example, the reaction (46)) of the diagram



where (A, Z-1)* is the excited nucleus (A, Z-1), and p and n denote a proton and a neutron. The amplitude of the process (49), naturally, depends on the elementary amplitude of the reaction $\pi^- + p \rightarrow n + \gamma$. In the final analysis, however, finding the amplitude (49) reduces to calculating the amplitude of the process



where the wavy line with the cross mark denotes an external field.

The dipole and spin-dipole external fields, generated in the processes (45)–(48), have the following tensor structure:

$$\sum_k f_k(q, r_k) Y_{1m}(n_k) \tau_{\pm}, \quad (51)$$

$$\sum_k f_k(q, r_k) (Y_1 \otimes \sigma)_{JM} \tau_{\pm}, \quad (52)$$

where Y_{1m} is the usual spherical harmonic, σ and τ_{\pm} are the spin and isospin Pauli matrices, and $f_{1,2}(q, r)$ are functions of the radius r and the transferred momentum q , whose form is determined by the specific reaction.

The fields (51) and (52) excite the nucleus differently. In the field (51), just like in the field of a dipole photon, transitions without spin flip are strongest, i.e., transitions of the type

$$j_i = l + \frac{1}{2} \rightarrow j_f = l + \frac{1}{2} + 1, \quad (53)$$

where $j_{i,f}$ are the total single-particle angular momenta at the start and at the end. The field (52) makes transitions with spin flip, i.e., the transitions

$$j_i = l - \frac{1}{2} \rightarrow j_f = l + 1 + \frac{1}{2}, \quad (54)$$

$$j_i = l + \frac{1}{2} \rightarrow j_f = l + 1 - \frac{1}{2}$$

stronger (for example, $1p_{1/2} \rightarrow 2d_{5/2}$, $1p_{3/2} \rightarrow 2d_{3/2}$). Correspondingly the field (51) excites the GDR state (true, it does so with a transferred momentum different than for the photon), while the field (52) excites the spin-dipole giant resonance state.

We shall now study examples of the manifestation of configurational splitting in the excitation spectra of nuclei in the reactions (45)–(48). Figure 22 shows the excitation spectrum of the ${}^6\text{Li}$ nucleus in the reactions (46)–(48), in which the spin-isospin branch of the excitation predominates. Since there are still no experimental data on the total photoabsorption cross section it is impossible to compare directly the purely dipole and spin-dipole excitation spectra. Figure 22 shows the measurements^{54,59} (histogram) and calculations in the BSM($1\hbar\omega$) approach^{54,60,61} of the radiative capture of pions from mesonic-atom orbits. The theory relates the appearance of the first (low-energy) peak with transitions of the nucleon within the outer unfilled 1p-shell, leading to final states with the Young scheme [42]. The theory relates the next maximum with the transitions of the nucleon in the outer 1p shell into the neighboring unfilled 0s shell and partially from the filled 0s shell into the unfilled 1p shell, but with the formation of a nuclear system with states with the Young scheme [33]. Finally, the third peak is due completely to transitions of the nucleon from a deep 0s shell, as a result of which the nuclear system is formed in states with the Young scheme [32].

The charge-exchange reaction (n,p) with a 60 MeV neutron results in an analogous excitation spectrum (see Fig. 22). The cross section in the region of the high-energy peak, which is greater than the cross section in the reaction (π^-, γ), is due to the contribution of purely dipole excitations, present in the (n, p) reaction at the energies used in the experiment.

Recent measurements⁵⁷ of the excitation spectrum of the nuclear system as a result of photoproduction of π^+ mesons on a ${}^6\text{Li}$ nucleus (see Fig. 22) also indicates the existence of structure in it. This structure fits into the theoretical picture following from the concept of configurational splitting. The angular distributions of the pions formed also can be explained starting from the predictions of the theory re-

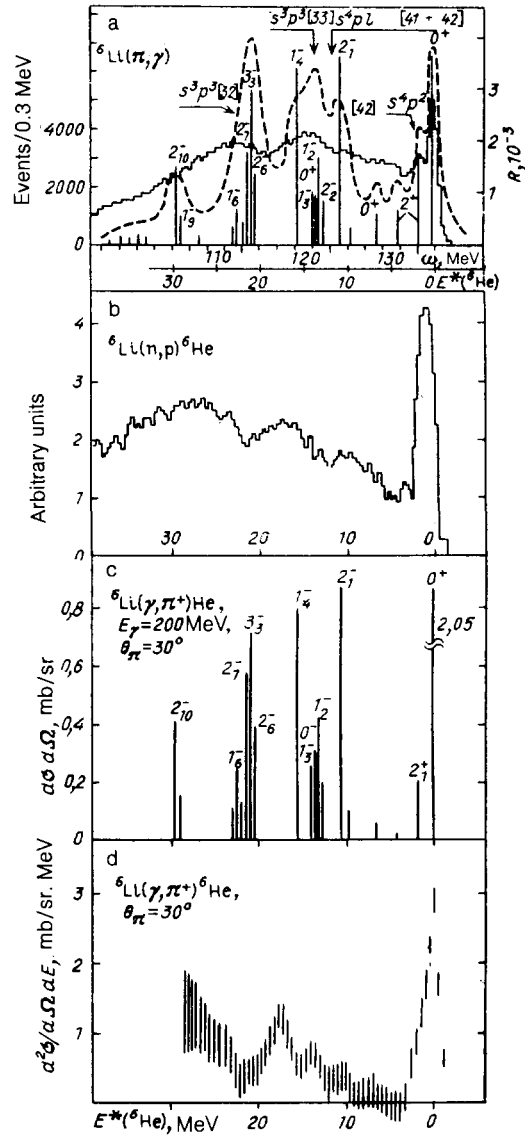


FIG. 22. The structure of the giant resonance in the ${}^6\text{Li}$ nucleus excited as a result of: radiative capture of pions [the histogram—experiment of Refs. 54 and 59, the vertical lines—calculations, the dashed line—calculations taking into account the smearing of individual peaks over an interval of width $\Delta E = 2$ MeV (Refs. 54, 60, 61)] (a), charge exchange of 60 MeV neutrons (experiment Refs. 51 and 56) (b), photoproduction of π^+ mesons (theory⁵⁸); vertical lines—differential cross section of individual resonances, integrated over their width (c) and photoproduction of π^+ mesons (experiment^{57,64}) (d).

garding the contribution of transitions of nucleons in different shells into a specific interval of excitation of the nuclear system—see Fig. 23, taken from Ref. 57. Thus in the region of excitation of the nuclear system from 12 to 14 MeV the contribution of nucleons in the outer shell, i.e., 1p-2d transitions, predominates, while in the energy range from 20 MeV and higher transitions from a deep shell, i.e., 0s \rightarrow 1p transitions, predominate.

We shall now study the ${}^7\text{Li}$ nucleus. In this nucleus it is possible to compare directly the structures of the excitation curves of the nuclear system in the photonuclear reaction

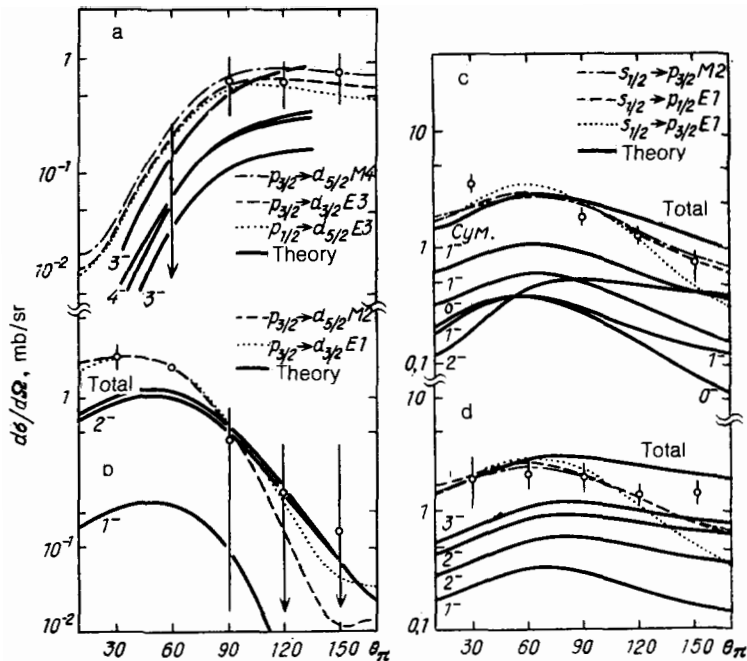


FIG. 23. The angular distribution of photopions for the ${}^6\text{Li}$ nucleus in four energy regions of excitation of the nuclear system:⁵⁸ E^* (MeV) = 12 (a), 13.6 (b), 17.7 (c), and 24 (d). Solid curves—Calculation in the BSM ($1\hbar\omega$) variant of the shell model,⁵⁸ the other curves correspond to single-particle calculations.⁵⁷ The experimental data are taken from Ref. 64, and the figure is taken from Ref. 64.

(Fig. 24)⁶² and the corresponding curves for radiative capture of pions from mesonic-atom orbits (Fig. 24c), and also as a result of photoproduction of pions (Fig. 24d). The curve in Fig. 24a was drawn in order to visualize the energy dependence. Like the case of excitation of ${}^6\text{Li}$ the purely dipole branch of the excitation extends to higher energies than the spin-dipole branch. The ratio of the peaks in the excitation spectrum of the nuclear system is also different. The theory of Refs. 54 and 61 attributes the appearance of the low-energy peak to transitions of an outer nucleon into a neighboring shell with the formation of a nuclear system in final states with the Young schemes [43] and [421]. The high-energy peaks are due to transitions of a nucleon from a deep 0s shell, resulting in states of the nuclear system with the Young scheme [331].

It follows from the examples presented above that all the experimental data taken together can be understood and interpreted based on the concept of configurational splitting of the dipole resonance.

In 1p-shell nuclei the dipole branch of the excitation extends up to much higher energies than the spin-dipole branch. A different situation is realized in 2s, 2d-shell nuclei. The strong nucleon transition $1p_{3/2} \rightarrow 2d_{3/2}$ results in a nuclear state with the configuration $|1p_{3/2}2d_{3/2} J^\pi = 1^-, T = 1\rangle$, which lies in the region of high excitations. Such a transition is manifested weakly in a photonuclear reaction and very strongly in the muon absorption reaction and backscattering of electrons, since it is connected with the flipping of the nucleon spin. The comparison made in Fig. 25 of the theoretical excitation spectra of the nuclear system for the example of the ${}^{32}\text{S}$ nucleus under conditions of photoabsorption, backscattering of electrons, and μ^- capture was made neglecting the spread in the high-energy resonance over states of a complicated nature.

Since the high-energy peak is related to the excitation of a nucleon from a deep 1p shell the decay of this peak will lead to highly excited states of the $(A - 1)$ nucleus (deep hole). In this connection there arises a very unique and complicat-

ed situation involving muon capture.⁶⁸ We shall discuss this situation in somewhat greater detail. This situation is shown schematically in Fig. 26 for the example of the ${}^{32}\text{S}$ nucleus. The absorption of muons by a $1p_{3/2}$ nucleon results in the formation of a ${}^{32}\text{P}$ nucleus with excitation energy above 20 MeV. Configurational splitting makes possible decay of the ${}^{32}\text{P}$ nucleus formed into states of the ${}^{31}\text{P}$ nucleus corresponding to the configuration $1\bar{p}_{3/2}(2s,2d)^4$. The parity of the levels of this configuration is different from that of the ground and low-lying states and the levels appear at 6–7 MeV (see, for example, Ref. 69). But this is higher than the threshold for subsequent ejection of a proton. Thus in (2s,2d)-shell nuclei configurational splitting leads to the fact that the channel (μ^-, ν_μ, n, p) should be observed^{67,68} with high intensity in muon capture (up to 15–20% of the total absorption of muons). The yield of charged particles should be appreciably higher in (2s,2d)-shell nuclei in 1p-shell nuclei, in which, neglecting mixing, such processes are forbidden.

All the experimental data taken together (see the data collected in the review of Ref. 7) indicate that the yield of charged particles produced by the absorption of muons is indeed maximum in 2s, 2d-shell nuclei and reaches about 20% per capture. Measurements of the yields of final nuclei show that two particles are predominantly ejected—a proton and a neutron.

Thus we can see that the concept of configurational splitting makes it possible to understand and interpret a large body of experimental data as a whole. A more thorough check of the concept and its consequences is possible only in more subtle and complicated experiments, which must include measurements of coincidences between different reaction products. This new level of data, undoubtedly, will make it possible to check fine details of the main concept, and thereby also the ideas about the structure and the mechanism of the interaction of different particles with light nuclei. We discussed such a program of research in Refs. 43 and 52. For this reason we shall not dwell on them here, and

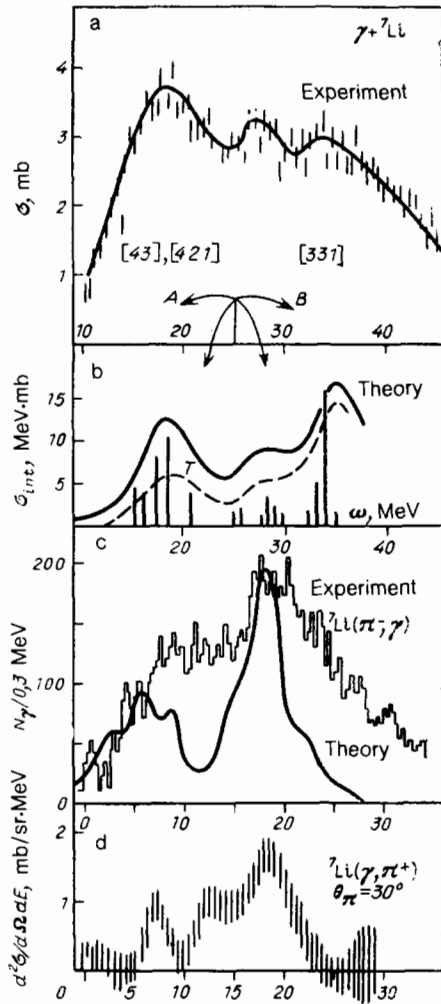


FIG. 24. The cross section for photoabsorption (a and b), radiative capture (c), and photoproduction of pions (d) for the ${}^7\text{Li}$ nucleus. a) Experiment⁶⁷ (the curve is drawn solely for visualization). b) The theory of Ref. 63 (the branch $T_{>}$ of the photonuclear resonance is singled out, solid line—calculation taking into account the smearing of individual resonances, which are shown in the form of vertical lines; the arrows mark the regions where nucleons of the outer (A) and inner (B) shells predominate; the Young schemes of the resonance states are presented). c) Radiative capture of pions from mesonic-atom orbits of ${}^7\text{Li}$ (histogram—experiment⁵⁴, solid line—theory^{54,61}). d) Photoproduction of π^+ mesons on ${}^7\text{Li}$ (experiment^{57,64}).

we refer the interested reader to the indicated works.

In conclusion we shall briefly discuss an interesting extension of the concept of configurational splitting. We are talking about energetically distinguished transitions with spin flip

$$j_i = l + \frac{1}{2} \rightarrow j_f = l + 1 - \frac{1}{2}$$

with $l = n$, where n is the principal quantum number, i.e., about transitions of the type

$$\begin{aligned} 1p_{3/2} &\rightarrow 2d_{3/2}, \\ 2d_{5/2} &\rightarrow 3f_{5/2}, \\ 3f_{7/2} &\rightarrow 4g_{7/2} \text{ and so on.} \end{aligned} \quad (55)$$

Such transitions are especially important in the analysis of the spin-dipole resonance. With no relation to the general problem of deep holes the energy of these transitions is significantly higher than the average energy of transitions

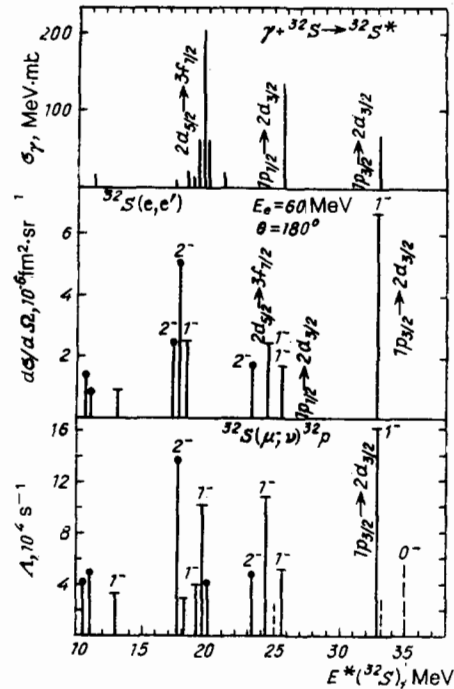


FIG. 25. The excitation spectrum of a nuclear system resulting from the absorption of muons⁶⁵ by the ${}^{32}\text{S}$ nucleus is compared with photoabsorption and backscattering of electrons⁶⁶ (theory).

between states of the neighboring shells n and $n + 1$. For example, in a heavy nucleus such as ${}^{208}\text{Pb}$ the energies of the transitions $4g_{9/2} \rightarrow 5h_{9/2}$, $5h_{11/2} \rightarrow 6i_{11/2}$ are equal to 11 and 12 MeV, respectively, and the average transition energy is equal to 7–8 MeV. The distinctive nature of the transitions (55) in the ${}^{16}\text{O}$ nucleus results in GDR with a “double hump” structure. The energy distinctive nature of the transitions (55) with respect to energy, of course, is associated

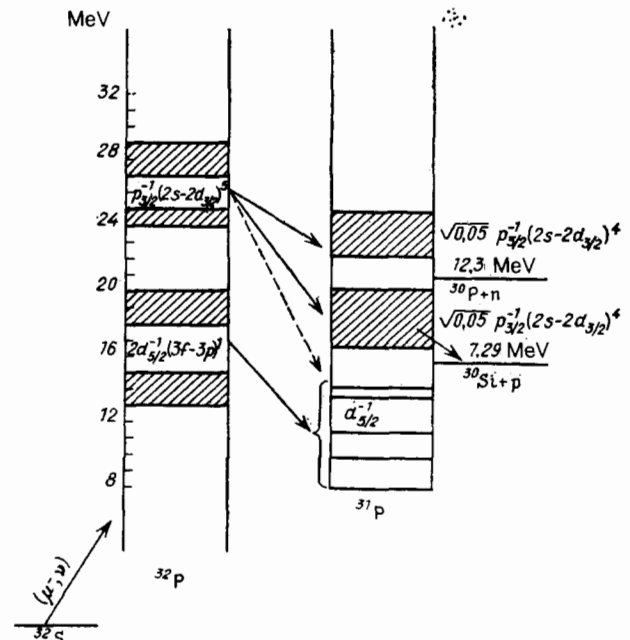


FIG. 26. A schematic representation of the excitation and decay of the ${}^{32}\text{S}$ nucleus in the process of muon capture.

with the spin-orbital part of the shell potential and in this sense can be interpreted as a manifestation of configurational splitting. Thus interpreting this term broadly we can say that the separate effects of configurational splitting can be traced in practically all nuclei.

5. CONCLUSIONS

In this review we analyzed the basic features of the physics of the giant dipole resonance in light nuclei—1p- and 2s, 2d-shell nuclei. The physics of the GDR in these nuclei is substantially different from the physics of the GDR in medium and heavy nuclei, and in this sense it is new. The heart of this new physics is configurational splitting, ultimately determined by the special properties of the mean (Hartree-Fock) nuclear field and thereby by the special properties of the nucleon-nucleon potential. Configurational splitting permits encompassing with one concept a very wide collection of properties of excited states of light nuclei, manifested in different reactions:

- a) "strange" variations of the width of the GDR—its enormous magnitude in nuclei at the start of a shell (${}^7\text{Li}$, ${}^9\text{Be}$, ${}^{23}\text{Na}$) and completely "normal" in nuclei heavier than ${}^{10}\text{B}$ and ${}^{28}\text{Si}$;
- b) the long tail of the GDR, extending right up to energies $\omega \approx 50$ MeV;
- c) the existence of two branches of the GDR, separated in energy, in 1p-shell nuclei—the pygmy resonance and the principal peak;
- d) predominant decay of 1p-shell nuclei into highly excited states of the final nuclei;
- e) the "double-hump" character of the ω dependence of the cross section of the (γ, γ) reaction in 2s, 2d-shell nuclei; and,
- f) the "multihump" structure of the excitation spectrum of final nuclei in muon capture reactions, radiative pion capture, and charge exchange between nucleons.

The main features of the phenomenon of configurational splitting were predicted theoretically at the Scientific-Research Institute of Nuclear Physics at Moscow State University; the theory was later confirmed experimentally by the work of the photonuclear group at the same institute and later by other photonuclear groups.

We can now state that without the concept of configurational splitting it is not possible to understand at all the "response" of light nuclei to different time-dependent external fields.

It should nonetheless be stressed that a detailed study of configurational splitting has yet to be performed. It will undoubtedly touch upon new physical effects and will require great efforts from experimentalists and theoreticians. In this connection we call attention to several big problems that must be solved.

First, the analysis of the partial cross sections of (γ, p) reactions on 2s, 2d-shell nuclei in the region of γ -ray energies greatly exceeding 30 MeV must be continued and analogous studies must be performed for the reaction (γ, n) . Such an analysis must be performed for 1p-shell nuclei.

Second, it is extremely important to identify the supermultiplet splitting in the GDR in 1p-shell nuclei based on the star-decay modes. Thus far such experimental studies are very fragmentary and unsystematic, even for the simplest nuclei ${}^6,7\text{Li}$ and ${}^9\text{Be}$.

Third, in order to trace in detail the universal features of configurational splitting it is necessary to perform coincidence experiments in reactions of radiative capture of pions from mesonic-atom orbits, μ capture, charge exchange between nucleons, etc.

Fourth, from a purely theoretical viewpoint, it is very important to determine the mechanisms of fragmentation of $1p_{3/2}$, 0s holes and to analyze the general reasons for the appearance of deep holes.

Finally, based on what was said above, we suspect that as the energy spread of the ph states decreases in the Hartree-Fock approximation (or as the off-diagonal elements of the ph interaction increase) a jump-like transition occurs from the "dispersed" ph states to a collective dipole state. It would also undoubtedly be interesting to study theoretically the question of the realization of this unique "phase transition."

¹The spectroscopic factor is the squared parentage coefficient $\langle \psi_i, j | \psi_0 \rangle^2$, multiplied by the number of "active" nucleons.

²The energy of "fouring" is lower than that indicated in Sec. 3.1 because here the "foured" nucleons are located in different shells (0s and 1p).

¹A. B. Migdal, Zh. Eksp. Teor. Fiz. **15**, 81 (1945).

²G. C. Baldwin and G. S. Klaiber, Phys. Rev. **71**, 3 (1947); **73**, 1156 (1948). M. L. Perlman and G. Friedlander, *ibid.*, 442. B. C. Diven and G. M. Almi, *ibid.* **80**, 407 (1950).

³M. Goldhaber and E. Teller, *ibid.* **74**, 1046 (1948).

⁴D. H. Wilkinson, Physica **22**, 1039 (1956).

⁵J. P. Elliot and B. H. Flowers, Proc. R. Soc. London **24**, 57, 75 (1957).

⁶G. E. Brown and M. Bolsterly, Phys. Rev. Lett. **3**, 472 (1959).

⁷V. G. Neudachin, V. G. Shevchenko, and N. P. Yudin, Zh. Eksp. Teor. Fiz. **39**, 108 (1960) [Sov. Phys. JETP **12**, 79 (1961)].

⁸P. M. Endt, Atomic Data Nuclear Data Tables **19**, 23 (1977). P. M. Endt and C. van der Leun, Nucl. Phys. A **310**, 1 (1978). F. A. Ajzenberg-Selove, *ibid.* **360**, 1 (1981); **413**, 1 (1984); **433**, 1 (1985).

⁹J. M. Cavedon, Phys. Rev. Lett. **40**, 978 (1982). T. de Forest and J. D. Walecka, Adv. Phys. **15**, 1 (1966). T. W. Donnelly and J. D. Walecka, Ann. Rev. Nucl. Sci. **25**, 329 (1975). T. W. Donnelly and I. Sick, Rev. Mod. Phys. **6**, 461 (1984).

¹⁰V. Amaldi, G. Campos Venturi, G. Cortellessa, G. Fronterotta, A. Reall, and P. Salvadori, Phys. Lett. **22**, 593 (1966). J. Mougey, M. Bernheim, A. Bussiere, A. Gillebert, Phan Xuan Ho, M. Priou, D. Royer, I. Sick, and G. I. Wagner, Nucl. Phys. A **262**, 461 (1976). K. Nakamura, S. Hiramatsu, T. Kamae, H. Muramatsu, and N. Izutsu, *ibid.* **271**, 221. J. Mougey, *ibid.* **335**, 35 (1980); **396**, 39 (1983). W. I. McDonald, *ibid.*, 463. S. Frullani and J. Mougey, Adv. Nucl. Phys. **15**, 1 (1983).

¹¹A. N. James, P. T. Andrews, P. Kirkby, and B. G. Lower, Nucl. Phys. A **138**, 145 (1969). G. Jacob and Th. A. J. Maris, Rev. Mod. Phys. **45**, 6 (1973). L. Antonuk, P. Kitching, C. A. Miller, D. A. Hutcheon, W. J. McDonald, G. C. Neilson, W. C. Olsen, and A. W. Stetz, Nucl. Phys. A **370**, 389 (1981).

¹²S. Fallieros, B. Goulard, and R. H. Venter, Phys. Lett. **19**, 388 (1965). N. Auerbach, T. Hufner, A. K. Kerman, and C. M. Shakin, Rev. Mod. Phys. **44**, 48 (1972). N. Auerbach, Phys. Rep. **98**, 278 (1983).

¹³A. B. Migdal, Theory of Finite Fermi Systems and Atomic Nuclei, Applications to Interscience, N. Y., 1967 [Russ. original, Nauka, M., 1965 and 1983]. S. V. Tolokonnikov and S. A. Fayans, Pis'ma Zh. Eksp. Teor. Fiz. **35**, 403 (1982) [JETP Lett. **35**, 499 (1982)]. J. Speth, E. Werner, and W. Wild, Phys. Rep. **33**, 127 (1977). J. Speth, V. Klemm, T. Wambach, and G. E. Brown, Nucl. Phys. A **343**, 382 (1980).

¹⁴V. V. Balashov and V. M. Chernov, Zh. Eksp. Teor. Fiz. **43**, 227 (1962) [Sov. Phys. JETP **16**, 162 (1963)]. M. Danos and W. Greiner, Phys. Rev. B **138**, 876 (1965). N. P. Yudin, Izv. Akad. Nauk SSSR, Ser. Fiz. **26**, 1222 (1962). [Bull. Acad. Sci. USSR Phys. Ser. **26**, 1234 (1962)]. F. A. Zhivopistsev, V. M. Moskovkin, and N. P. Yudin, *ibid.* **30**, 306 (1966) [*ibid.* **30**, 311 (1966)].

¹⁵G. F. Bertsch, Phys. Lett. B **80**, 61 (1978).

¹⁶A. I. Vdovin and V. G. Solov'ev, Fiz. Elem. Chastits At. Yadra **14**, 237 (1983) [Sov. J. Part. Nucl. **14**, 99 (1983)].

¹⁷M. G. Urin, *ibid.* **15**, 245 [*ibid.* **15**, 109 (1984)].

¹⁸H. Feshbach, A. Kerman, and S. Kronin, Ann. Phys. **125**, 429 (1980).

¹⁹J. Bardeen, L. N. Cooper, and J. R. Schrieffer, Phys. Rev. **108**, 1175 (1957). N. N. Bogolyubov, Zh. Eksp. Teor. Fiz. **34**, 58 (1958) [Sov.

- Phys. JETP 7, 41 (1958)]. S. T. Belyaev, K. Dan. Vidensk. Selsk. Mat.-Fys. Med. 31, No. 11 (1959). V. G. Solov'ev, *ibid.*
- ²⁰V. G. Neudachin, V. G. Shevchenko, and N. P. Yudin, Phys. Lett. 10, 180 (1964). V. G. Neudachin and V. G. Shevchenko, *ibid.* 12, 18.
- ²¹A. Bohr and B. R. Mottelson, Nuclear Structure, Vol. 1, Benjamin, N. Y., 1969 [Russ. transl., Mir, M., 1971, Vol. 1].
- ²²a) V. Gillet, Nucl. Phys. 51, 410 (1964). b) V. Gillet and N. Vinh-Mau, *ibid.* 54, 321. c) M. Gavinato, M. Marangoni, and A. M. Saruis, Phys. Lett. B 163, 49 (1985).
- ²³B. S. Dolbilkin, V. I. Korin, L. E. Lazareva, and F. A. Nikolaev, Pis'ma Zh. Eksp. Teor. Fiz. 1 (5), 47 (1965) [JETP Lett. 1, 148 (1965)].
- ²⁴R. Bergere, Photonuclear Reaction 1, Lect. Notes Phys. 61, 1 (1977).
- ²⁵R. G. Allas, S. S. Hanna, L. Meyer-Schutzmeister, R. E. Segel, P. P. Singh, and Z. Vager, Phys. Rev. Lett. 13, 187 (1964).
- ²⁶L. Rosenfeld, Nuclear Forces, North-Holland, Amsterdam, 1948. T. H. R. Skyrme, Philos. Mag. 1, 1043 (1956). D. Vautherin and D. M. Brink, Phys. Rev. C 5, 626 (1972). M. Maroquer, K. Heyde, and G. Wenes, Nucl. Phys. A 404, 269, 298 (1983).
- ²⁷K. A. Brueckner, R. J. Eden, and N. C. Francis, Phys. Rev. 99, 76 (1955). T. T. S. Kuo and G. E. Brown, Nucl. Phys. 85, 40 (1966). J. W. Negele, Phys. Rev. C 1, 1260 (1970).
- ²⁸R. F. Barret, L. C. Biedeharn, M. Danos, P. P. Delsanto, W. Greiner, and H. G. Washweiler, Rev. Mod. Phys. 45, 44 (1973). M. Cavinato, M. Marangoni, P. L. Ottaviani, and A. M. Saruis, Nucl. Phys. A 444, 13 (1985).
- ²⁹H. Feshbach, Ann. Phys. (N.Y.) 5, 357 (1958). V. V. Balashov, Nucl. Phys. A 129, 369 (1969). C. Mahaux and H. A. Weidenmuller, Shell-Model Approach to Nuclear Reactions, North-Holland, Amsterdam, 1969. I. Rotter, Fiz. Elem. Chastits At. Yadra 6, 435 (1975); 15, 762 (1984) [Sov. J. Part. Nucl. 6, 175 (1975); 15, 341 (1984)].
- ³⁰J. J. Griffin, Phys. Rev. Lett. 17, 478 (1966); Phys. Lett. B 24, 5 (1967). H. Feshbach, Rev. Mod. Phys. 46, 1 (1974). M. Blann, Ann. Rev. Nucl. Sci. 25, 123 (1975). D. Agassi, H. A. Weidenmuller, and G. Mantzouronis, Phys. Rep. 22C, 147 (1975). W. A. Friedman, M. S. Hussein, K. W. McVoy, and P. A. Mellow, *ibid.* 77, 48 (1981). F. A. Zhivopistsev and V. G. Sukharevskii, Fiz. Elem. Chastits At. Yadra 15, 1208 (1984) [Sov. J. Part. Nucl. 15, 539 (1989)].
- ³¹E. P. Wigner and L. Eisenbud, Phys. Rev. 72, 242 (1947). A. M. Lane and R. G. Thomas, Rev. Mod. Phys. 30, 257 (1958). A. G. Sitenko, Theory of Nuclear Reactions [in Russian], Energoizdat, M., 1983.
- ³²D. J. Thouless, Nucl. Phys. 22, 78 (1961). G. E. Brown, L. Castillejo, and J. A. Evans, *ibid.* 1, 27, 323.
- ³³D. Pines and P. Nozière, The Theory of Quantum Liquids, Benjamin, N. Y., 1966 [Russ. transl., Mir, M., 1967]. M. J. Amusia and N. A. Cherpokov, Case Stud. At. Phys. 5, 47 (1975).
- ³⁴C. B. Dover and Nguyen Van Giai, Nucl. Phys. A 190, 373 (1972). D. Vautherin and D. M. Brink, Phys. Rev. C 5, 626 (1972). C. Mahaux and H. Ngo, Nucl. Phys. A 410, 271 (1983).
- ³⁵G. M. Vagradov and V. V. Gorchakov, Fiz. Elem. Chastits At. Yadra 5, 308 (1974) [Sov. J. Part. Nucl. 5, 122 (1974)].
- ³⁶G. D. Mahan, Phys. Rev. 163, 1097 (1969). P. Nozieres and S. I. Dominicus, *ibid.* 178, 1097.
- ³⁷L. Majling, J. Rizek, Yu. I. Bely, V. G. Neudachin, and N. P. Yudin, Nucl. Phys. A 143, 429 (1970).
- ³⁸B. S. Ishkhanov and I. M. Kapitonov, The Physics of the Atomic Nucleus and Elementary Particles [in Russian], TSNIIatominform, M., 1983, Part 3, p. 18.
- ³⁹B. S. Ishkhanov and I. M. Kapitonov, Pis'ma Zh. Eksp. Teor. Fiz. 42, 465 (1985) [JETP Lett. 42, 576 (1985)].
- ⁴⁰B. S. Ishkhanov and I. M. Kapitonov, Decay Properties of the Giant Resonance of 23, 2d-Shell Nuclei. Report on Scientific-Research Work [in Russian], Scientific-Research Institute of Nuclear Physics at Moscow State University, M., 1985.
- ⁴¹V. V. Varlamov, I. M. Kapitonov, V. I. Shvedunov, and A. V. Shumakov, Prib. Tekh. Eksp., No. 6, 30 (1980) [Instrum. Exp. Tech. (USSR) 23, 1347 (1980)].
- ⁴²I. M. Kapitonov, Author's Abstract of Doctoral Dissertation in Physical-Mathematical Sciences, Scientific-Research Institute of Nuclear Physics at Moscow State University, M., 1983.
- ⁴³R. A. Eramzhyan, B. S. Ishkhanov, I. M. Kapitonov, and V. G. Neudachin, Phys. Rev. 136, 229 (1986); Fiz. Elem. Chastits At. Yadra 12, 905 (1981); 14, 286 (1983) [Sov. J. Part. Nucl. 12, 362 (1981); 14, 119 (1983)].
- ⁴⁴V. V. Varlamov, B. S. Ishkhanov, I. M. Kapitonov, A. N. Panov, and V. I. Shvedunov, Izv. Akad. Nauk SSSR, Ser. Fiz. 43, 186 (1979) [Bull. Acad. Sci. USSR. Phys. Ser. 43].
- ⁴⁵E. Kerkhove, R. van de Vyver, H. Ferdinande, D. Ryckbosch, P. van Otten, P. Berkvens, and E. van Camp, Phys. Rev. C 32, 368 (1985).
- ⁴⁶S. G. Nilsson, J. Sawicki, and N. Glendenning, Nucl. Phys. 33, 239 (1962). B. S. Ishkhanov, I. M. Kapitonov, V. G. Shevchenko, and B. A. Yuryev, Phys. Lett. 9, 162 (1964). B. Forkman and W. Steifler, Nucl. Phys. 56, 615 (1964).
- ⁴⁷N. G. Goncharova, Kh. R. Kissener, and R. A. Eramzhyan, Fiz. Elem. Chastits At. Yadra 16, 773 (1985) [Sov. J. Part. Nucl. 16, 337 (1985)]. R. I. Hughes, R. H. Sambell, E. G. Muirhead, and B. M. Spicer, Nucl. Phys. A 238, 189 (1975). N. G. Goncharova and N. P. Yudin, Yad. Fiz. 12, 725 (1970) [Sov. J. Nucl. Phys. 12, 392 (1970)].
- ⁴⁸P. E. Hodgson, Rep. Prog. Phys. 38, 846 (1975).
- ⁴⁹H. Weyl, The Classical Groups, Princeton University Press, Princeton, N. J. 1986 [Russ. transl. IL, M., 1947]. M. Hamermesh, Group Theory and Its Applications to Physical Problems, Addison-Wesley, Reading, MA, 1962 [Russ. transl., Mir, M., 1966].
- ⁵⁰A. N. Boyarkina, The Structure of 1p-Shell Nuclei [in Russian], Izd. Mosk. Univ., M., 1973.
- ⁵¹S. Ferroni, B. Mosconi, G. Piragino, and V. Wataghin, Nucl. Phys. 76, 58 (1977).
- ⁵²V. V. Balashov, G. Ya. Korenman, and R. A. Eramzhyan, Absorption of Mesons by Atomic Nuclei [in Russian], Atomizdat, M., 1978.
- ⁵³G. Gmitro, Kh. R. Kissener, P. Tryuol', and R. A. Eramzhyan, Fiz. Elem. Chastits At. Yadra 13, 1230 (1982) [Sov. J. Part. Nucl. 13, 513 (1982)].
- ⁵⁴M. Gmitro, Kh. R. Kissener, P. Tryuol', and R. A. Eramzhyan, *ibid.* 14, 773 (1983).
- ⁵⁵F. Petrovich and W. G. Love, Nucl. Phys. A 354, 499 (1981).
- ⁵⁶F. P. Brady, G. Needham, Y. I. Ullmann, C. M. Castaneda, T. I. Ford, N. S. P. King, J. L. Romero, M. L. Webb, V. A. Brown, and C. H. Poppe, J. Phys. G 10, 363 (1984).
- ⁵⁷K. Shoda, "Electromagnetic interactions of nuclei at low and medium energies" (in Russian) in: Proceedings of the 6th Seminar at the Institute of Nuclear Physics of the Academy of Sciences of the USSR, Moscow, 1986, p. 118.
- ⁵⁸S. S. Kamalov, T. D. Kaipov, and R. A. Eramzhyan, *ibid.*, p. 143; Z. Phys. Kl. A 322, 321 (1985).
- ⁵⁹D. Renker *et al.*, Phys. Rev. Lett. 41, 1279 (1978).
- ⁶⁰R. A. Sakaev and R. A. Eramzhyan, Joint Institute of Nuclear Research Report R2-9610, Dubna, 1976.
- ⁶¹H. R. Kissener, G. E. Dogatar, R. A. Eramzhyan, and R. A. Sakaev, Nucl. Phys. A 312, 394 (1978).
- ⁶²J. Ahrens *et al.*, *ibid.* 251, 479 (1975).
- ⁶³H. R. Kissener and R. A. Eramzhyan, in Proceedings of the International Conference on Nuclear Physics with Electromagnetic Interactions: Abstracts of Contributed Papers, Mainz, 1979, p. 20.
- ⁶⁴K. Shoda, O. Sasaki, S. Toyama, H. Tsubota, T. Kobayashi, and A. Kagaya, in International Symposium on Weak and Electromagnetic Interactions in Nuclei: Contributed Papers, Heidelberg, 1986.
- ⁶⁵Yu. I. Bely, R. A. Eramzhyan *et al.*, Nucl. Phys. A 204, 357 (1973).
- ⁶⁶Yu. I. Bely and N. M. Kabachnik, Yad. Fiz. 14, 1113 (1971) [Sov. J. Nucl. Phys. 14, 619 (1972)].
- ⁶⁷R. A. Eramzhyan, L. Majling, and I. Rizek, Nucl. Phys. A 247, 411 (1975).
- ⁶⁸R. A. Eramzhyan, L. Majling, and I. Rizek, Czech. J. Phys. B 3, 482 (1981).
- ⁶⁹P. M. Endt and C. van der Leun, Nucl. Phys. A 310, 1 (1978).
- ⁷⁰Yu. A. Batusov and R. A. Eramzhyan, Fiz. Elem. Chastits At. Yadra 8, 229 (1977) [Sov. J. Part. Nucl. 8, 95 (1977)].

Translated by M. E. Alferieff